Kinematics of autowave structures in excitable media

V. A. Davydov, V. S. Zykov, and A. S. Mikhaĭlov

Moscow Institute of Radio Engineering, Electronics, and Automation
Institute of Problems in Control, Academy of Sciences of the USSR, M. V. Lomonosov State University, Moscow

(Submitted 17 April 1991)
Usp. Fiz. Nauk **161**, 45–85 (August 1991)

We consider an approximate approach to the description of complex space-time structures in different types of excitable media based on the kinematics of autowave fronts. Because of the generality and relative simplicity of the kinematic approach, it is possible to obtain analytical results for different types of autowave motion in two and three-dimensional excitable media. The kinematic approach is used to treat steady-state autowave structures and also to study the evolution of autowaves in inhomogeneous, time-dependent and anisotropic media.

INTRODUCTION

Modern physics is finding it increasingly necessary to use fundamentally nonlinear models to explain a wide class of natural phenomena. Examples of fundamentally nonlinear effects are so-called *self-organization processes*, which occur in the formation, evolution, and decay of complex space-time structures. The study of self-organization processes is of great current interest in diverse physical, chemical, and biological systems.[25,51,55,57,115,123,125] This rapidly developing interdisciplinary field is called synergetics.[48,49,63]

Dramatic examples of the phenomenon of self-organization are self-excited waves (or autowaves, for short) in so-called *excitable media*.[15,46] A distributed excitable medium consists of locally coupled active elements which can form a pulse in response to an external signal. Pulses propagating in excitable media are often called autowaves, since their characteristics (shape, velocity, and so on) are mainly determined by the parameters of the medium and are practically independent of the initial conditions and boundary conditions.

Examples of excitable media are nerve and muscle tissues in living organisms,[42] certain solutions of chemical reactants,[8,24,25] solid-state electronic systems,[6,19,60] magnetic superconductors,[13] ecological systems,[59] and so on.

A rotating spiral wave is a typical example of an autowave in a two-dimensional medium. Spiral waves are observed in solutions with Belousov–Zhabotinskiĭ reactants,[65,102,103,121] (Fig. 1), colonies of microorganisms,[82] in the retina of the eye,[69,83] and in the tissues of the heart muscle.[66,72,123]

In three-dimensional media autowave structures are observed in the form of cylindrical rolls or vortex rings.[45,46,122,125] When these waves interact with one another the result can be three-dimensional structures with very complicated topology.[126]

The currently accepted mathematical model of an excitable medium is a system of parabolic equations of the "reaction—diffusion" type

$$\frac{\partial \mathbf{U}}{\partial t} = \hat{D}\Delta \mathbf{U} + \mathbf{F}(\mathbf{U}), \tag{1.1}$$

where U is the state vector of an elementary volume of the excitable medium. In a chemical medium the components of the vector **U** are the concentrations of the reactants, the matrix $\hat{D}$ represents their diffusion coefficients, and the nonlinear function $F(\mathbf{U})$ specifies the frequency of chemical reactions in each elementary volume. In other types of media the components of the vector **U** might be the temperature or electric potential, while the elements of the matrix $\hat{D}$ might be the thermal conductivities or the specific electrical conductivities.

Real excitable media are normally described by the multicomponent system of equations (1.1). However, numerous studies[32,123,130] show that the basic features of autowave structures can be reproduced in the framework of the two-component system

$$\frac{\partial E}{\partial t} = D_E \Delta E + F(E, g),$$
$$\frac{\partial g}{\partial t} = D_g \Delta g + \varepsilon G(E, g). \tag{1.2}$$

The "excitable property" of the system (1.2) is determined by the saw-tooth form of the nonlinear function F. The function G can be monotonic or even linear. The function $F(E,g)$ is usually specified by polynomials or by piecewise linear functions.[78,105,108,110,111,117] As an example, we show in Fig. 2 the piecewise linear function $F(E,g)$ first suggested in Ref. 47 and is often used to study autowave structures.[23,32,54,94,106] This function is given by the expression

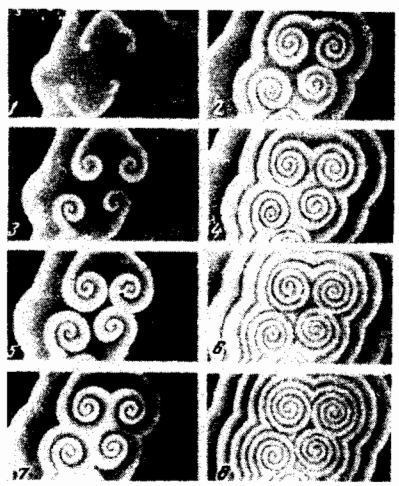

FIG. 1. Formation of a spiral wave as a result of rupture of the front of a concentric wave in a Belousov–Zhabotinskiĭ reaction.

 0038-5670/91/080665-20$01.00

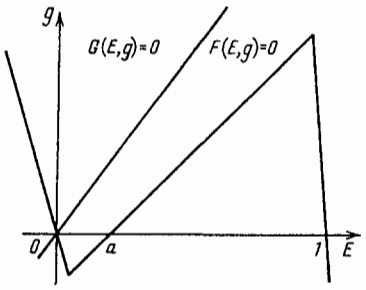

FIG. 2. Piecewise-linear approximation of the null-isoclines of the model (1.2).

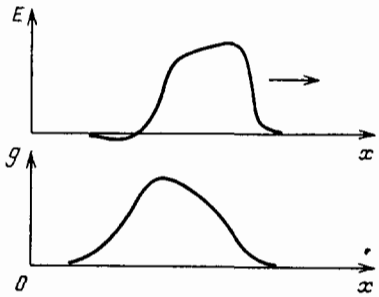

FIG. 3. Autowave profile in a two-component model of an excitable medium.

$$F(E, g) = f(E) + g, \tag{1.3}$$

where

$$\begin{aligned} f(E) &= -Ek_1, \quad E < \sigma, \\ &= (E - a)k_f, \quad \sigma \le E \le 1 - \sigma, \\ &= (1 - E)k_2, \quad 1 - \sigma < E, \end{aligned}$$

$$k_1 = \frac{a - \sigma}{\sigma} k_f, \; k_2 = \frac{1 - \sigma - a}{\sigma} k_f.$$

The function $G(E,g)$ is given by

$$\begin{aligned} G(E, g) &= k_g E - g \quad (k_g E - g \geqslant 0), \\ &= k_\varepsilon (k_g E - g) \quad (k_g E - g < 0). \end{aligned} \tag{1.4}$$

The limiting case of the system (1.2) when $\varepsilon = 0$ is effectively a one-component system with two stable states. In a system of this kind one can have transition waves from one stable state to the other. These types of waves have been used to describe "gene diffusion"[43] and flame propagation.[27,62]

In the more general case of (1.2) with $\varepsilon \neq 0$ there exists a single equilibrium state ($E = 0, g = 0$), which is stable to small perturbations. Above-threshold perturbations in the system generate a propagating pulse whose leading front corresponds to a transition wave from the state of rest to an excited state, and whose trailing front corresponds to a return of the system to the initial state (Fig. 3).

It is important to note that the shape of the pulse and its propagation velocity asymptotically approach steady values independent of the initial conditions.

We see from Fig. 3 that just because the variable E (often called the activator) approaches the value $E = 0$, this does not mean that the system has returned to its initial state. The second component g (called the inhibitor) differs strongly from the steady state over a certain time interval. It follows from the solution of (1.2) with $\varepsilon = 0$ and $g > 0$ (Ref. 53) that the increase in the slow variable g near the autowave front leads to a decrease in the propagation velocity of the autowave until it stops completely and begins to propagate in the opposite direction. There are two important consequences of this property of the structure of an autowave pulse. The first is that pulses propagating in opposite directions cancel one another out. The second is that the velocity of a periodic train of pulses is smaller than the velocity of a single pulse and it decreases as the period between pulses decreases (this property of an excitable medium is related to dispersion). In addition, when the period between pulses is less than a certain minimum value $T_{\min}$, steady propagation of the train of pulses becomes impossible. If the period T between pulses is large compared to $T_{\min}$, then the interaction between the pulses (i.e. the response time of the medium) can be neglected and the train can be considered as a set of single pulses.

A large number of experimental data on excitable media are available and there have been numerous computer simulations of the reaction–diffusion model. The basic problems of the theory of autowave structures are to explain the data from a unified point of view and to propose new directions of experimental research.

It is important to note that the time evolution of an autowave structure can be completely determined by describing only the time dependence of the position of the wave front. This idea drastically simplifies the treatment of autowave processes and is the basis of the kinematic approach to autowave structures considered in the present review article.

This idea was first formulated in Ref. 119 and was later extended and applied to the so-called axiomatic models,[5,17,18,44,76,77,109,112] in which the motion of autowave fronts is specified heuristically based on the results of autowave processes in one-dimensional models of the reaction–diffusion type. Because of this extreme simplification, the application of the axiomatic models to two and three-dimensional media often leads to disagreements with experiment and with simulation results.

Obviously two and three-dimensional excitable media are of the most practical interest, and autowave processes in these media are much more complicated and diverse than in one-dimensional media. In the case of two and three-dimensional media the kinematic approach discussed below shows its superiority over other approximate methods in that it is general and relatively simple. The kinematic approach is not limited to steady-state autowave structures, but can also be used for time-dependent problems.

2. BASIC PROPERTIES OF THE MOTION OF AUTOWAVE FRONTS

The velocity and shape of a steady-state wave in a one-dimensional medium described by (1.2) with $D_g = 0$ are found by introducing the change of variables $\xi = -x + V_0 t$. Then

$$\begin{aligned} D_E \frac{\partial^2 E}{\partial \xi^2} &= V_0 \frac{\partial E}{\partial \xi} - F(E, q), \\ V_0 \frac{\partial g}{\partial \xi} &= \varepsilon G(E, g). \end{aligned} \tag{2.1}$$

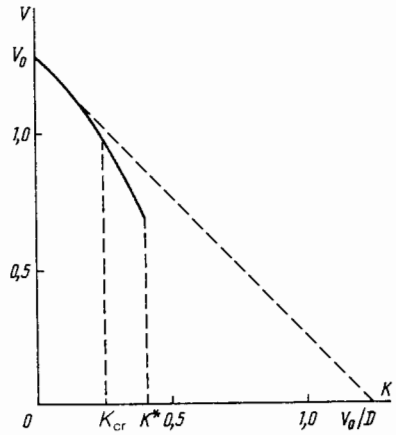

FIG. 4. Dependence of the propagation velocity of an autowave on the curvature of its front for the model (1.2) with $k_f = 1.7$, $k_g = 2.0$, $d = 0$, $\sigma = 0.01$, $k_\varepsilon = 0.01$, and $\varepsilon = 0.35$.

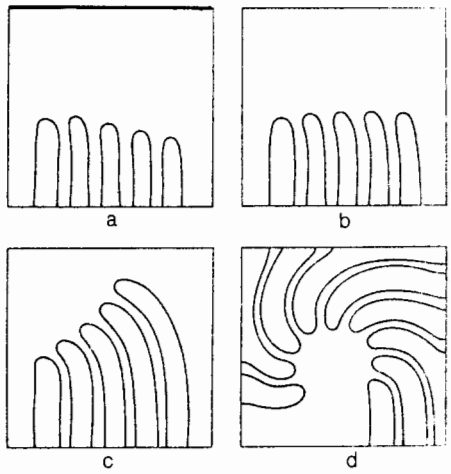

FIG. 5. Evolution of the edge of a wave with a rectangular front in the model (1.2) for different excitabilities of the medium. a) $\varepsilon = 0.4$, b) 0.388, c) 0.35, d) 0.3.

Because of the small parameter ε in this system, we can use the perturbation method.[70] We note that (2.1) has two solutions. One solution represents a pulse propagating with a velocity V_0 which is close to the velocity V_{00} in the same system with $\varepsilon = 0$. In the first approximation

$$V_0 = V_{00} - V_1\varepsilon\,, \tag{2.2}$$

where $V_1 > 0$.

The second solution represents a pulse whose velocity V^n is much smaller than V_0. This solution is unstable[70,78] and is not observed in physical systems.

When ε increases, the velocity of the stable pulse decreases and the velocity of the unstable pulse increases. When $\varepsilon = \varepsilon_{cr}$ the two solutions join into one, and when $\varepsilon > \varepsilon_{cr}$ steady propagation of a pulse in the system (1.2) is no longer possible.

The system (2.1) also describes the propagation of a rectangular autowave in a two-dimensional excitable medium. However, in the two-dimensional case the propagation velocity of the front depends on its curvature.[9,26,95] Indeed, steady-state motion of a wave front with curvature K is described by the system of equations[37,41]

$$D_E\frac{d^2E}{d\xi^2} = (V - D_EK)\frac{dE}{d\xi} - F(E, g)\,,$$
$$V\frac{dg}{d\xi} = \varepsilon G(E, g). \tag{2.3}$$

The propagation velocity V of a pulse in (2.3) will obviously depend on the curvature of the front K. It was shown in Ref. 30 that $V(K)$ can be expressed in terms of the function $V_0(\varepsilon)$:

$$V(K) = V_0\left(\varepsilon\frac{V - D_Ek}{V}\right) + D_EK\,. \tag{2.4}$$

Using (2.2), we can transform (2.4) to the form

$$V(K) = \frac{1}{2}\left(V_{00} - V_1\varepsilon - D_Ek\right) + \left[\frac{1}{4}\left(V_{00} - V_1\varepsilon - D_EK\right)^2 - V_1\varepsilon D_EK\right]^{1/2}. \tag{2.5}$$

It follows from (2.5) that the propagation velocity of a convex front decreases as its curvature increases (Fig. 4). It is easy to show that for small curvatures

$$V(K) = V_0 - D_E(V_{00} + V_1\varepsilon)\,[(V_{00} - V_1\varepsilon)K]^{-1}. \tag{2.6}$$

When $K > K^*$ steady-state propagation of the front is no longer possible. The limiting value of the curvature of the front $K = K^*$ is given by

$$K^* = [(V_{00} - V_1\varepsilon) + 2(V_{00}V_1\varepsilon)^{1/2}]D_E^{-1}\,. \tag{2.7}$$

Therefore analysis of (1.2) shows that the propagation velocity of the wave depends on the curvature of its front and demonstrates the existence of a critical curvature beyond which steady propagation of a convex front is impossible. These conclusions are supported by experimental data.[79] However, they do not restrict the propagation of autowaves in a two-dimensional medium.

Since the medium is in the same state of rest before the arrival of an excitation wave and after the system leaves the excited state and returns to the initial state, an autowave in a two-dimensional medium can have a free edge (break) not in contact with the boundary of the medium. For example, a free edge exists near the core of a spiral wave (Fig. 1). Obviously the evolution of the free edge of the autowave must be taken into account in its kinematics.

Calculation of the motion of a half-wave for the model (1.2) shows that the evolution of the edge depends on the excitability of the medium in an essential way (Fig. 5). If the excitability of the medium is small ($\varepsilon = 0.4$) the half-wave contracts (Fig. 5a). When the excitability of the medium is sufficiently high ($\varepsilon = 0.35$) the half wave is elongated (Fig. 5c). Elongation and distortion of the wave form can lead to the formation of a spiral wave (Fig. 5d) rotating about a circular region (the core), which remains unperturbed.

We note that a spiral wave results in a periodic train of excitation pulses through all points of the medium, except within the core. Therefore the propagation velocity of the wave fronts will depend not only on their curvature, but also on the period of rotation T of the spiral. When the period of

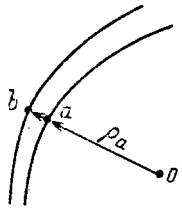

FIG. 6. Diagram used in the derivation of the fundamental equation of kinematics.

rotation $T \gg T_{\min}$ the dependence of propagation velocity on T can be neglected and the kinematics of the motion of the autowave can be derived by taking into account only the curvature dependence of the velocity of the wave front.

3. KINEMATIC EQUATIONS

The mathematical model forming the basis of the kinematic approach takes into account the basic features of the motion of autowave fronts in excitable media discussed above. We consider an arbitrary smooth curve lying in a plane. The curve is assumed not to intersect itself and it represents the wave front. We note that this curve effectively has an "obverse" and "reverse", i.e. at each point one of the two directions normal to the curve is in a consistent way. Each segment of the curve moves along the direction of the preferred normal with velocity V. The edge of the front (if it exists) moves along the normal, but also experiences a steady tangential "growth" or contraction with velocity C.

Any curve lying in a plane can be specified by its natural equation $K = K(l)$ relating the arc length l and curvature K at a given point.[56] Because the front is moving, its curvature will obviously also depend on the time t: $K = K(l,t)$.

We consider the position of the wave front at a certain time t. Suppose its curvature at point a in Fig. 6 is equal to K_a at time t. During the time dt a small neighborhood of point a on the front moves to the neighborhood of point b and the curvature at this point is K_b. We find a relation between K_a and K_b. It is convenient to use polar coordinates with the origin at the center of curvature of a small element of the front near point a. Then we have the relation

$$\rho_b = \rho_a + V dt, \tag{3.1}$$

where $\rho_a = 1/K_a$ is the radius of curvature at point a and ρ_b is the polar radius at point b. The curvature of a curve specified in polar coordinates by the equation $\rho = \rho(\phi)$ is

$$K = (\rho^2 - 2\rho'^2 - \rho\rho'')(\rho^2 + \rho'^2)^{-3/2}, \tag{3.2}$$

where a prime implies differentiation with respect to ϕ. Substituting (3.2) into (3.1), we obtain, to within terms of order dt

$$K_b = K_a - \left(VK_a^2 + K_a^2 \frac{\partial^2 V}{\partial \phi^2}\right) dt \tag{3.3}$$

(here we have used the fact that $\partial \rho_a / \partial \phi = 0$, since ρ_a is the radius of curvature at point a). Transforming to differentiation with respect to arc length l ($dl = \rho_a d\phi$) in (3.3), we obtain

$$K_b - K_a = dK = -\left(K_a^2 V + \frac{\partial^2 V}{\partial l^2}\right) dt. \tag{3.4}$$

On the other hand, $dK = (\partial K/\partial l)dl + (\partial K/\partial t)dt$. It is not difficult to obtain the following expression for the increment of arc length dl after time dt

$$dl = \left(\int_0^l KV d\xi\right) dt + C dt. \tag{3.5}$$

The first term in (3.5) represents the increase in the arc length due to a change in the radii of curvature at each point on the curve. The second term corresponds to an increase in arc length due to growth of the front at its free edge, which is chosen to lie at a distance l from the origin.

Combining (3.4) and (3.5), we obtain the equation

$$\frac{\partial K}{\partial l}\left(\int_0^l KV d\xi + C\right) + \frac{\partial K}{\partial t} = -K^2 V - \frac{\partial^2 V}{\partial l^2}, \tag{3.6}$$

which is called the fundamental equation of kinematics of autowave fronts on a plane surface. It was first obtained in Ref. 28, but for a long time it was used only for steady-state motion of autowave fronts.[29,30,32] The specific feature of the steady-state case is that there is no growth or contraction of the free edge of the wave front.

For non-steady-state motion of autowaves the growth of the front at the end point of the wave plays a very important role. This process was first described quantitatively in Ref. 22, where it was noted that if the interaction between the fronts is neglected, then the velocity C of the tangential displacement of the free edge should depend only on the curvature of the front K_0 near it: $C = C(K_0)$, where

$$K_0 = \lim_{l \to 0} K(l).$$

Computer simulations show (see Fig. 5) that a change in the excitability of the medium can cause contraction of the free edge to turn into growth. Since a distortion in the front of an autowave is equivalent in a certain sense to a change in the excitability of the medium (see Sec. 2), the tangential displacement of the free edge of the wave changes direction at a certain value of the curvature K_{cr} near the end point. This property of the function $C(K_0)$ is reproduced by a linear function of the form

$$C = \gamma(K_{cr} - K_0), \ \gamma > 0. \tag{3.7}$$

The dependence of the propagation velocity of the front of an autowave on its curvature (Sec. 2) can also be represented by a linear function

$$V = V_0 - DK. \tag{3.8}$$

A sufficient condition for the applicability of the linear approximation (3.8) is

$$p \equiv \frac{DK_{cr}}{V_0} \ll 1. \tag{3.9}$$

The natural equation describes only the position of the curve on the plane. To describe completely the displacement of the front it is sufficient to specify the motion of any point on the front with respect to a given coordinate system. It is convenient to choose the free edge of the front for this purpose. For example, let x_0 and y_0 be the Cartesian coordinates

of the end point in the plane and let α_0 be the angle between the tangent vector to the front at the point $l = 0$ and the X axis. Then we have the following equations of motion:

$$\dot{x}_0 = -V(l = 0) \sin \alpha_0 - C \cos \alpha_0,$$
$$\dot{y}_0 = V(l = 0) \cos \alpha_0 - C \sin \alpha_0, \tag{3.10}$$

$$\dot{\alpha}_0 = \frac{\partial V}{\partial l}\Big|_{l=0} + CK_0 . \tag{3.11}$$

The first term on the right hand side of (3.11) is the rate of change of the angle α_0 due to the different propagation velocities at different points on the front, while the second term is due to a slow growth of the free edge.[10,11,21,22]

Equations (3.6)–(3.8), together with (3.10) and (3.11), are a complete system of equations for the form and motion of an autowave front with an edge. Hence in the kinematic approach an excitable medium is characterized by a small number of phenomenological parameters: V_0, K_{cr}, D, γ. These parameters must be obtained from experiment or by solution of (1.2), which are "microscopic" equations from the point of view of kinematics. It turns out that in a number of cases the values of certain of the coefficients do not depend on the specific forms of the functions $F(E,q)$ and $G(E,g)$ in (1.2). For example, if the diffusion coefficient of the inhibitor D_g is equal to zero, then the coefficient D is equal to the diffusion coefficient of the activator to within terms of order ε [see (2.6)]. If $D_E = D_g$, then $D = D_E = D_g$ and the coefficient γ vanishes.[10]

It is simple to extend this model to the case when the autowave propagates on a curved surface, rather than on a plane. In this case K will be the geodesic curvature of the front on the surface. We derive the fundamental equation of kinematics in this more general case, following Ref. 11.

If we take a series of snapshots of the propagation of a single autowave front on a two-dimensional surface, we obtain a succession of positions of the front, i.e. a one-parameter family of curves with the time t as a parameter. We introduce a curvilinear orthogonal coordinate system (ϕ,t), in which the coordinate lines $t = \text{const}$ coincide with the fronts of the autowave at time t. In this coordinate system the first quadratic form (the square of the differential arc length) has the form

$$ds^2(t, \phi) = V^2(t, \phi)dt^2 + B^2(t, \phi)d\phi^2, \tag{3.12}$$

where V and B are the Lamé coefficients and V is obviously the velocity of normal propagation of the front. The Gaussian curvature of the surface can be expressed through the Lamé coefficients as[52]

$$\Gamma = -\frac{1}{VB}\left[\left(\frac{B_t}{V}\right)_t + \left(\frac{V_t}{B}\right)_\phi\right], \tag{3.13}$$

where the subscripts t and ϕ denote the corresponding partial derivatives. The geodesic curvature K (the curvature on the surface) of a coordinate line can also be expressed in terms of the Lamé coefficients (Ref. 52): $K = B_t/VB$. Then using (3.13), we have

$$\Gamma = -K^2 - \frac{1}{V}\frac{\partial K}{\partial t} - \frac{1}{VB}\frac{\partial}{\partial \phi}\left(\frac{1}{B}\frac{\partial V}{\partial \phi}\right). \tag{3.14}$$

We next transform from the variable ϕ to the length of the front l. It follows from (3.12) that $dl = B\,d\phi$. Then (3.14) is transformed to the new variables with the help of the relation $d/dt \to \partial/\partial t + (dl/dt)\partial/\partial l$, where

$$\frac{dl}{dt} = \int_{\phi_0}^{\phi} B_t d\phi = \int_{\phi_0}^{\phi} KVB d\phi = \int_0^l KV d\xi , \tag{3.15}$$

and growth of the front can be taken into account by adding the velocity C to the right hand side of (3.15). In terms of the new variables we finally obtain from (3.14)

$$\frac{\partial K}{\partial l}\left(\int_0^l KV d\xi + C\right) + \frac{\partial k}{\partial l} + K^2 V + \frac{\partial^2 V}{\partial l^2} = -\Gamma V. \tag{3.16}$$

This equation is the fundamental equation of kinematics of an autowave front on a curved surface with Gaussian curvature Γ. In the special case of a plane ($\Gamma = 0$) (3.16) reduces to (3.6).

The relation (3.16) must be supplemented by the equations of motion of the free edge of the front analogous to (3.10) and (3.11). The form of these equations depends on the choice of coordinate system on the curved surface.

In spite of the fact that the fundamental equations of kinematics (3.6) and (3.16) are nonlinear partial integro-differential equations for the function $K(l,t)$, we will see that they are much easier to solve than the "microscopic" equations (1.2). In addition, it is important to note that these equations can be applied not only to autowaves, but also to other evolution processes. For example, (3.6) was obtained in Ref. 67 independently of earlier papers[11,28] and used to describe the growth of dendrites. The specific features of the problem under consideration are introduced by replacing (3.8) with a different relation between the propagation velocity of the front V and its curvature K.[68] The fundamental equation (3.6) with the velocity (3.8) was later used in Ref. 99 to describe the time dependence of dual spiral waves. However, the growth velocity C was not calculated using (3.7), but was set equal to a constant. This assumption obviously cannot provide even a qualitative description of non-steady-state autowave processes.

4. STEADY CIRCULATION OF SPIRAL AUTOWAVES ON A PLANE

Equation (3.6) has the trivial steady-state solution $K(l,t) \equiv 0$ for $l \geqslant 0$, which corresponds to a plane front with an edge moving forward with velocity V_0. However this solution is unstable to small perturbations. Numerical analysis of (3.6) shows[39,73] that regardless of the form of the small initial perturbation, a plane half-wave always turns into a spiral wave rotating about a fixed center with a constant angular velocity (see Fig. 7). The basic characteristics of the steady-state circulation of a spiral wave can be calculated analytically using (3.6).

In the case of steady-state circulation the form of the wave front is constant. Only the position of the curve in the plane changes in time. Therefore K does not depend on t. In addition, in steady-state circulation the free edge of the wave does not grow or contract, since in the steady-state case the curvature of the wave front near the free edge $K(l = 0) \equiv K_0$ has reached the critical value K_{cr}, and therefore $C \equiv 0$ from (3.7).

Since $\partial K/\partial t \equiv 0$ and $C \equiv 0$, (3.6) can be integrated once to obtain[11,29]

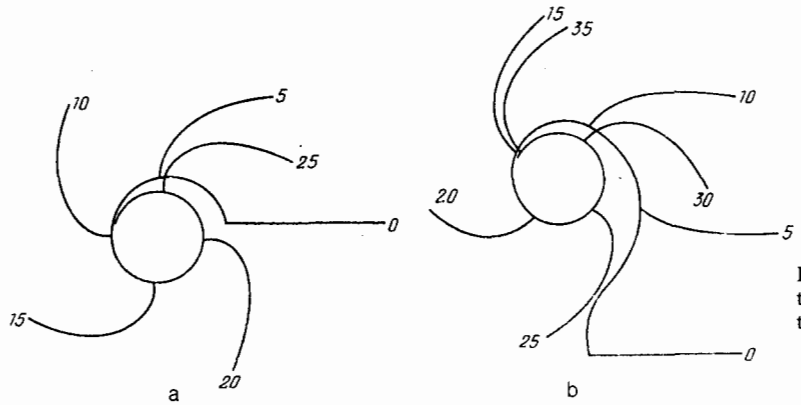

FIG. 7. Evolution of a rectilinear front in the kinematic model of the motion of an excitation wave for different initial perturbations. a) $K(0,0) = 0.1\,K_{cr}$, b) $-0.1\,K_{cr}$.

$$K\int_0^l KV\,d\xi - D\frac{dK}{dl} = \omega\,. \tag{4.1}$$

The integration constant ω is the angular velocity of the spiral wave. This follows from (3.11), since $C = 0$, while $dV/dl = -D\,dK/dl$ [see (3.8)].

To obtain analytical solutions of (4.1) we first assume D vanishes. Then (4.1) has the solution

$$K = (\omega/2V_0 l)^{1/2}\,. \tag{4.2}$$

Note that $R = V_0/\omega$ is the radius of a circle (the boundary of the core of the spiral wave) along which the free edge of the front moves. Hence the wave front is given by the natural equation

$$K = (2Rl)^{-1/2}\,, \tag{4.3}$$

which describes the involute of the circle. When $l \gg R$ it becomes an Archimedean spiral with a pitch equal to $h = 2\pi R$.

This result was obtained in the classic paper of Ref. 119. Later it was rederived in Ref. 122, where it was emphasized that the curvature of the front $K \to \infty$ when $l \to 0$ [see (4.2)]. Hence the dependence of the velocity of the front on its curvature cannot be neglected for small l, i.e. near the boundary of the core.

We next calculate the parameters of a spiral wave when the velocity of the front depends on its curvature. The frequency of rotation of the spiral wave $\omega = \omega_0$, which appears in (4.1) as an unknown parameter, can be found as follows. Far from the center of the spiral the curvature must approach zero, i.e. $K \to 0$ when $l \to \infty$. As noted above, the curvature K_0 near the free edge of the front is equal to K_{cr}. The solution of interest must therefore satisfy the two boundary conditions

$$K(0) = K_{cr}\,, \quad \lim_{l\to\infty} K(l) = 0\,. \tag{4.4}$$

Since (4.1) is a first-order equation, the two boundary conditions (4.4) can be satisfied simultaneously only for a certain value of ω_0. Hence (4.1), together with the boundary conditions (4.4), is a nonlinear eigenvalue problem whose solution gives the frequency ω_0.

This problem was solved numerically in Refs. 29, 32, and 37. The following form for ω approximately fits the numerical results:

$$\omega = V_0 K_{cr}\psi(p)\,, \tag{4.5}$$

where

$$\psi(p) = c_1 p^{1/2} - c_2 p - c_3 p^2\,, \tag{4.6}$$

and $c_1 = 0.685$, $c_2 = 0.06$, and $c_3 = 0.293$.

According to (4.5), the angular velocity of a spiral wave increases with increasing K_{cr}. It follows from (3.8), however, that K_{cr} cannot exceed V_0/D. Therefore the maximum value of ω is reached when $K_{cr} = V_0/D$, which corresponds to $p = 1$. In this case the velocity of normal propagation of the free edge of the wave vanishes. This special case was first considered in Ref. 7 to describe the growth of spiral dislocations in crystals. The angular velocity of a spiral dislocation $\omega = 0.33 V_0 K_{cr}$ obtained in Ref. 7 is in close agreement with (4.6) with $p = 1$.

Another important special case is $p \ll 1$, which corresponds to a weakly excitable medium. An approximate analytical calculation for this case was given in Ref. 22 based on "matching" the interior and exterior solutions. This is one of the methods of solving singular perturbed equations where the highest derivative in the equation is multiplied by a small parameter.[16] Indeed, when l is sufficiently large the derivative term on the left hand side of (4.1) can be neglected. The solution in this region is given by (4.2). On the other hand, it follows from (4.1) that when $l = 0$ the derivative $dK/dl = -\omega_0/D$. Therefore for small l the natural equation of the wave front has the form

$$K = K_{cr} - \frac{\omega_0}{D} l\,. \tag{4.7}$$

The expressions (4.2) and (4.7) are the exterior and interior approximations to a single phase trajectory and therefore they must be matched in some way. We require that the values of the two functions and their first derivatives must match at a certain point $l = l_0$. These conditions give two equations:

$$K_{cr} - \omega_0/Dl_0 = \left(\frac{2V_0 l_0}{\omega}\right)^{-1/2}\,, \tag{4.8}$$

$$\frac{\omega_0}{D} = \frac{1}{2}\left(\frac{2V_0}{\omega_0}\right)^{-1/2} l_0^{-3/2}\,. \tag{4.9}$$

Their solution has the form

$$\omega_0 = \left(\frac{2}{3}\right)^{3/2} (DV_0)^{1/2} K_{cr}^{3/2}\,, \tag{4.10}$$

$$l_0 = \frac{1}{2}\left(\frac{3}{2}\right)^{1/2}\left(\frac{D}{K_{cr}V_0}\right)^{1/2}\,. \tag{4.11}$$

We note that the results of this approximate analytical treatment are in good agreement with the results of numerical integration of (4.1). Indeed, when $p \ll 1$ we obtain from (4.5) the angular velocity

$$\omega_0 = \xi (DV_0)^{1/2} K_{cr}^{3/2}, \quad \xi = 0.685, \tag{4.12}$$

which differs from (4.10) only by the more accurate value of the numerical constant. To within terms of order $p = DK_{cr}/V_0$ the radius of the core of the spiral wave can be calculated from the condition $\omega_0 R_0 = V_0$, which gives

$$R_0 = \xi^{-1} \left(\frac{V_0}{D}\right)^{1/2} K_{cr}^{-3/2}. \tag{4.13}$$

We now discuss these results. Clearly, when $K_{cr} \to 0$ the rotation frequency of the spiral wave ω_0 approaches zero and the radius R_0 of the core diverges. Except for a narrow layer with a width of order l_0 near the core boundary, the spiral wave front has the form of an involute of a circle of radius R_0 and is given by (4.3) with $R = R_0$. The width of the boundary layer is small compared to the core radius: $l_0/R_0 \sim p = DK_{cr}/V_0 \ll 1$.

The form of a spiral wave rotating around an aperture is also described by (4.1). However, note that the edge of the spiral wave moves along the boundary of the aperture, which is nonpermeable to diffusion and therefore is not free. The curvature of the edge can exceed K_{cr}. Nevertheless it must remain smaller than the critical curvature K^* for a continuous front [see (2.7) and Fig. 4]. Therefore the radius R^* of the smallest aperture for which a spiral wave can circulate along its boundary can be found by replacing K_{cr} by K^* in (4.13):

$$R^* = \xi^{-1} \left(\frac{V_0}{D}\right)^{1/2} (K^*)^{-3/2}. \tag{4.14}$$

When the radius is less than R^*, the edge of the wave breaks off from the aperture and the rotation frequency suddenly jumps to the lower value ω_0. This effect has been observed in a numerical simulation of the reaction–diffusion model.[107]

We also note that a spiral wave rotating concentrically inside of a circle of radius R_{cr} obeys the same kinematic equation (4.1), but the boundary conditions are no longer given by (4.4).[32] In this case the normal velocity of the front on the boundary of the circle must satisfy the condition

$$V(K_b) = \omega R_b, \tag{4.15}$$

which also determines the curvature of the front at the point of contact. Hence the rotation velocity of the spiral wave increases with decreasing radius R_{cr}.

In the kinematic model used here it has been assumed that the velocity V depends only on the local curvature of the front K, i.e. $V = V(K)$. In general, the velocity V of the front near its free edge will also depend on the arc length l: $V = V(l)$. The basic features of spiral waves were considered in Ref. 11 taking this dependence into account. It is found that this effect does not lead to essential differences, and we do not discuss it in detail here.

We note also that we have neglected the response time of the medium, which causes the propagation velocity of the waves to depend on the time interval T between them. This dependence is extremely important for the quantitative characteristics of spiral waves and also for many very important qualitative effects. Keener and Tyson[92,118] started from this dependence in constructing a theory of steady-state spiral waves, while the effect of the curvature of the front was taken into account as a correction. In the kinematic approach discussed here, we assume the opposite order: we first describe the spiral wave neglecting the dispersive properties of the medium, and then refine this description by introducing dispersion (see Sec. 9). In the case of steady-state circulation both approaches naturally lead to the same result: the velocity of the front is a function of the two parameters $V = V(K,T)$. However, the advantage of our approach becomes apparent in the case of non-steady-state autowave processes, which are not amenable to treatment by the alternative approach.

5. THE QUASISTEADY APPROXIMATION

The fundamental kinematic equation of autowave fronts (3.6) can also be used to describe different types of non-steady-state processes. Assume that we have introduced a small perturbation in the form of the front of a uniformly rotating spiral wave and that the perturbation is localized at a distance l from the free edge. We see from (3.6) that it will move away from the center of the wave toward the periphery, and at the same time it will spread out and attenuate because of "diffusion" with the diffusion coefficient D. According to (3.6) the velocity of this drift can be estimated as $K_{cr} V_0 l$ near the free edge, where $K \approx K_{cr}$.

Therefore a perturbation localized at the distance l moves with a velocity of order $K_{cr} V_0 l$ and its width grows as $(Dt)^{1/2}$. We consider the following question: at what distance must an initially localized perturbation be such that it can reach the free edge of the wave in spite of its drift? A necessary condition to reach the free edge is that over a certain interval of time the width of the perturbation $L_{dif} \approx (Dt)^{1/2}$ must exceed the distance between its center and the free edge of the wave $L_c \approx l + K_{cr} V_0 lt$. Comparison of these two quantities shows that L_{dif} can be larger than L_c only when the initial distance l does not exceed a quantity of order $(D/K_{cr} V_0)^{1/2}$. But according to (4.11) the width of the boundary layer near the core boundary is of this order.

It follows that the motion of the end point can be affected only by perturbations of the front originating within a narrow boundary layer at a distance of order l_0 from the free edge. The perturbation damps out after a time of order

$$\tau_D \approx \frac{l_0^2}{D} \approx (K_{cr} V_0)^{-1}. \tag{5.1}$$

We note that the relaxation time τ_D of a perturbation in the shape of the front in a weakly excitable medium is always much smaller than the period of circulation of the spiral wave.[10] Indeed, it follows from (4.12) and (5.1) that

$$\omega \tau_D \sim p^{1/2} = (DK_{cr}/V_0)^{1/2} \ll 1. \tag{5.2}$$

When the coefficient γ in (3.7) is equal to zero, growth does not occur and the quantity K_0 remains constant with time. In this case a spiral wave achieves a steady state after a time of order τ_D. The rotation frequency of the wave can be found from (4.12) by substituting K_0 for K_{cr}.

If γ is nonzero and positive, then growth or contraction of the front is accompanied by a time variation of K_0 such that the difference between K_0 and K_{cr} damps out within a

relaxation time τ_c. If γ is sufficiently small, $\tau_c \gg \tau_D$ and a quasi-steady-state regime is established.

In the quasi-steady-state regime the shape of the front near the core of a spiral wave can adjust itself adiabatically to the instantaneous value of the curvature $K_0(t)$ at the free edge, and this curvature in turn slowly varies because of growth or contraction. It is not difficult to show that the equation describing this variation in the quasi-steady-state regime can be obtained from (3.6) and has the form[10]

$$\frac{\partial k}{\partial t}\Big|_{l=0} = -c\frac{\partial k}{\partial l}\Big|_{l=0}. \tag{5.3}$$

The derivative $(\partial K/\partial l)_{l=0}$ is given by [see (4.7)]

$$\frac{\partial k}{\partial l}\Big|_{l=0} = -\omega/D, \tag{5.4}$$

Hence in the quasi-steady-state case the curvature K_0 at the free edge is time dependent and obeys the following first-order ordinary differential equation:

$$\frac{dK_0}{dt} = -\xi\gamma\left(\frac{V_0}{D}\right)^{1/2} K_0^{3/2}(K_0 - K_{cr}). \tag{5.5}$$

For small perturbations $\delta K_0 = K_0 - K_{cr}$ this equation can be linearized:

$$\frac{d\delta K_0}{dt} = -\frac{\delta K_0}{\tau_c}, \tag{5.6}$$

where the relaxation time τ_c is

$$\tau_c = D/\gamma\omega_0. \tag{5.7}$$

Using (5.1), (5.2), and (5.7), we obtain the following condition for the applicability of the quasi-steady-state approximation:[10]

$$\frac{\gamma}{D} \ll \left(\frac{V_0}{DK_{cr}}\right)^{1/2} = p^{-1/2}. \tag{5.8}$$

For typical excitable media the coefficient γ is between zero and a quantity of order D. Therefore since $(V_0/DK_{cr})^{1/2} \gg 1$, the condition (5.8) is nearly always satisfied and the quasi-steady-state approximation is valid.

To describe completely the evolution of a spiral wave in the quasi-steady-state approximation, (5.5) must be supplemented by additional equations determining the time dependence of the position of the end point of the front in the plane and the orientation of the front. As noted above, the motion of the end point is described by (3.10). The orientation of the front is specified by the angle α_0 of inclination of the tangent to the front at the end point. This angle obeys (3.11). When (5.8) is satisfied this equation simplifies, since then $(\partial V/\partial l)|_{l=0} = \omega$, where ω is found from (4.12) by replacing K_{cr} with K_0. Therefore (3.11) becomes

$$\dot{\alpha} = \xi\left(\frac{V_0}{D}\right)^{1/2} K_0^{3/2} + \gamma K_0(K_{cr} - K_0). \tag{5.9}$$

In the quasi-steady-state approximation the motion of a spiral wave is therefore described by a system of four first-order ordinary differential equations: (5.5), (3.10), and (5.9). These equations are much simpler than the fundamental kinematic equation (3.6), not to mention the initial "microscopic" system of reaction–diffusion equations.

6. RESONANCE AND DRIFT OF SPIRAL WAVES ON A FLAT SURFACE

By varying the parameters of the medium we can change its excitability and therefore the quantity K_{cr}. Suppose this quantity varies periodically in time according to the equation

$$K_{cr}(t) = K_{cr} + K_1\cos(\omega_1 t + \phi), \tag{6.1}$$

where $K_1 \ll K_{cr}$ and the modulation frequency ω_1 is close to the eigenfrequency ω_0 of the spiral wave. The periodic time dependence of K_{cr} leads to a periodic variation of the velocity of growth C [see (3.7)], which will be accompanied by a periodic variation in the curvature K_0 near the edge. The result is a periodic variation in the angular velocity. Modulation of the growth velocity and rotation frequency will lead to motion of the center of the spiral wave.

The characteristics of this motion are conveniently calculated in the quasi-steady-state approximation.[21] With the help of (6.1), equation (5.5) for $K_0(t)$ takes the form

$$\frac{dK_0}{dt} = \frac{\gamma}{D}\bar{\omega}_0\left(\frac{K_0}{K_{cr}}\right)^{3/2}(K_{cr} + K_1\cos(\omega_1 t + \phi) - K_0), \tag{6.2}$$

where $\bar{\omega}_0 = \xi(DV_0)^{1/2}K_{cr}^{3/2}$. Since $K_1 \ll K_{cr}$, the solution of (6.2) can be written in the form $K_0 = K_{cr} + \delta K_0(t)$, where $\delta K_0 \ll K_{cr}$. Keeping only terms of first order in δK_0 in (6.2) and assuming that $|\bar{\omega}_0 - \omega_1| \ll \bar{\omega}_0$, we obtain the following time dependence of the curvature $K_0(t)$ near the free edge of the front:

$$K_0(t) = K_{cr} + K_1\frac{\gamma/D}{1 + (\gamma/D)^2}\left[\sin(\omega_1 t + \phi) + \frac{\gamma}{D}\cos(\omega_1 t + \phi)\right].$$

Substituting this expression into (5.9), it is not difficult to find the time dependence of the angle α_0. Then the motion of the end point of the spiral wave (and hence the core center) can be calculated from (3.10). Omitting the laborious but straightforward calculations, we give the final result:[21] when the curvature varies periodically according to (6.1), the center of the core of the spiral wave moves with the velocities

$$\begin{aligned}\dot{X}_c &= v\cos[(\omega_1 - \bar{\omega}_0)t + \phi + \sigma],\\ \dot{Y}_c &= -v\sin[(\omega_1 - \bar{\omega}_0)t + \phi + \sigma],\end{aligned} \tag{6.3}$$

where

$$v = \frac{3}{4}V_0\frac{K_1}{K_{cr}}\frac{\gamma/D}{[1 + (\gamma/D)^2]^{1/2}}, \tag{6.4}$$

$$\sigma = \arccos[1 + (\gamma/D)^2]^{1/2}. \tag{6.5}$$

It follows from (6.3)–(6.5) that the core center of the spiral wave moves along a circle of radius

$$R_c = \frac{(3/4)V_0(K_1/K_{cr})\gamma/D}{|\omega_1 - \bar{\omega}_0|[1 + (\gamma/D)^2]^{1/2}}. \tag{6.6}$$

The radius grows as ω_1 approaches the eigenfrequency ω_0 (resonance). The velocity v is proportional to the modula-

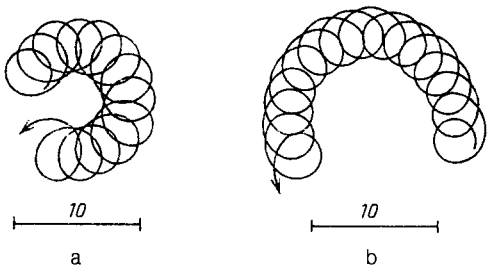

FIG. 8. Trajectories of the end point of a spiral wave obtained in the model (1.2) for a periodic modulation of the parameter ε with frequency ω_1. a) $\omega_1 = 0.23$, b) 0.255. The angular velocity of the spiral wave is $\omega_0 = 0.24$.

tion amplitude K_1. When ω_1 and $\bar{\omega}_0$ are exactly equal (perfect resonance) the core center moves with the constant velocity (6.4) along a straight line and the direction of motion is determined by the initial phase of the modulation ϕ and by the direction of rotation of the spiral wave (clockwise or counterclockwise).

Analytical calculations of resonance drift of a spiral wave are supported by computer simulations of the reaction–diffusion model[21] (Fig. 8).

Resonance of spiral waves is also observed experimentally using the light-sensitive Belousov–Zhabotinskiĭ reaction.[31] A spiral wave is first created in the medium. Then the illumination of the solution is varied periodically, which leads to a periodic modulation of the excitability. The wave pattern is photographed at equal time intervals against a background of fixed reference lines. Figure 9 shows a sequence of photographs (a–c) of a spiral wave with a time interval of 10 min and perfect resonance (the modulation period is exactly equal to the natural period of rotation of the wave). We see that the center of rotation moves with a constant velocity along one of the reference lines; the total displacement is 2 cm.

If two spiral waves are created in the medium with opposite directions of rotation, the initial phase of the modulation can be chosen in such a way that the centers of the two waves move toward one another and annihilate one another.[3]

We next consider drift of a sprial spiral wave in a nonuniform excitable medium. This effect has been studied repeatedly in computer simulations[21,58,87] and in experiments with Belousov–Zhabotinskiĭ chemical reactions. However, a satisfactory theory of this effect does not exist. Below we consider drift in the framework of the kinematic approach.[21,73]

Suppose K_{cr} varies slowly along the x direction, so that the change in K_{cr} over the core radius R_0 is small

$$\partial K_{cr}/\partial x \ll K_{cr}/R_0 . \tag{6.7}$$

As the spiral wave moves in the nonuniform medium its free edge passes through regions of the medium with different values of K_{cr}. Therefore the end point moves as if the critical curvature were time dependent:

$$K_{cr}(t) = K_{cr}(x_0 + R\cos\omega_0 t) = K_{cr} + bR_0\cos\omega_0 t\,, \tag{6.8}$$

where x_0 is the position of the center of the spiral wave along the x axis, $K_{cr} = K_{cr}(x_0)$, and $b = (\partial K_{cr}/\partial x)_{x=x_0}$.

Therefore the drift of a spiral wave in a weakly nonuniform medium reduces to the problem considered above of resonance with perfect coincidence of the frequencies and zero initial modulation phase ϕ_0. Substitution of (6.8) into (6.3)–(6.5) leads to an expression for the drift velocity.[21,73] The center of the spiral wave slowly moves along a straight line at an angle θ to the x axis. The drift velocity is equal to

$$v_{dr} = \frac{(3/4)V_0}{[1+(D/\gamma)^2]^{1/2}}\frac{R_0}{K_{cr}}\left|\frac{\partial K_{cr}}{\partial x}\right|, \tag{6.9}$$

and the tangent of the angle θ is given by

$$\mathrm{tg}\theta = -\frac{\gamma}{D}. \tag{6.10}$$

A change in the sign of the angular velocity ω_0 results in a change in sign of the component of the drift velocity along the y axis. But the direction of motion along the x axis remains the same. In particular, (6.10) shows that the drift of a spiral wave can be used to determine the coefficient γ of the excitable medium.

We note that drift of a spiral wave cannot continue for very long. In an infinite medium the core of a spiral wave sooner or later drifts into a region where the kinematic de-

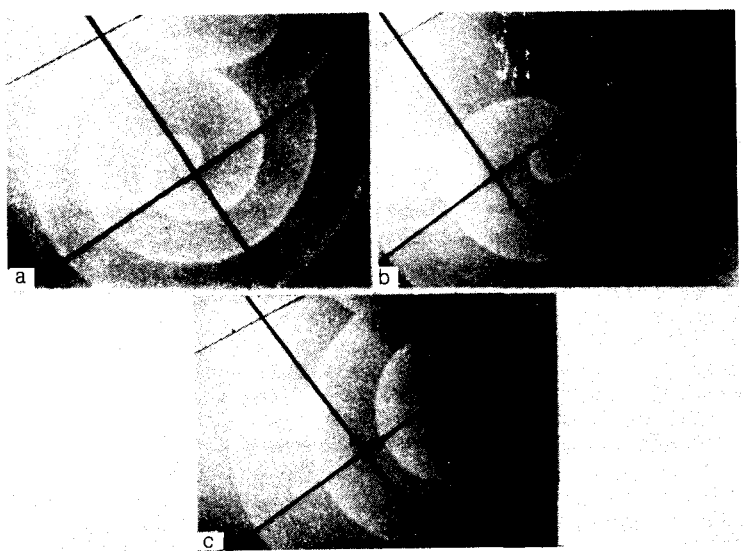

FIG. 9. Movement of the core center of a spiral wave in an experiment using a light-sensitive Belousov–Zhabotinskiĭ reaction.

scription is inapplicable because the conditions (6.7) or (3.9) no longer hold, for example. We emphasize, however, that the dimensions of the medium are small in experiments using Belousov–Zhabotinskiĭ reactions and also in computer simulations. Drifting with a constant velocity, the spiral wave hits the boundary of the medium and vanishes.

We have considered the most interesting effects associated with circulation of spiral waves in nonuniform and non-steady-state media. If the properties of the medium depend both on the coordinates and the time, i.e. the medium is both in a non-steady-state situation and is nonuniform, then the motion of spiral waves has new qualitative features. For example, in a medium with a periodically varying inhomogeneity gradient, resonance (i.e. motion of the core center along a straight line) is possible at twice the circulation frequency, while resonance at frequency ω_0 does not occur.[2]

It is interesting to note that resonance and drift of spiral waves also occur in so-called λ-ω systems. This important class of nonequilibrium media is also described by systems of equations of the reaction–diffusion type with spiral wave solutions.[84–86] But because of a number of important differences, the kinematic approach as described here cannot be used to consider this problem,[49] and study of resonance effects in λ-ω systems required development of special methods.[4]

7. SPIRAL WAVES IN ANISOTROPIC EXCITABLE MEDIA

In studying autowave processes in excitable media one normally considers only isotropic media. However, many excitable media (such as semiconductor systems, biological tissues, and so forth) are basically anisotropic. Therefore the study of autowave structures in anisotropic media is of great interest.

In an anisotropic medium the diffusion coefficients form a tensor $\hat{D}$. In the principal axis system of the tensor $\hat{D}$ the system of reaction–diffusion equations (1.2) on a plane with $D_g = 0$ takes the form

$$\frac{\partial E}{\partial t} = F(E, g) + D\frac{\partial^2 E}{\partial x^2} + D_1\frac{\partial^2 E}{\partial y^2}, \qquad \frac{\partial g}{\partial t} = \varepsilon G(E, g). \tag{7.1}$$

We introduce new spatial coordinates $x' = x$, $y' = y\lambda$, where $\lambda = (D/D_1)^{1/2}$. In terms of these coordinates the system of equations (7.1) reduces to (1.2) and therefore in the new coordinate system the medium is isotropic and the diffusion coefficient is equal to D. Hence we can study the motion of an autowave in an anisotropic medium by using a "primed" coordinate system in which the medium is isotropic. The solution is then transformed back to the initial "laboratory" system.

For example, it is not difficult to obtain the dependence of the velocity of a plane autowave front in an anisotropic medium on its propagation direction:[20]

$$V_0(\theta) = V_0(\lambda^2\cos^2\theta + \sin^2\theta)^{1/2}\lambda^{-1}, \tag{7.2}$$

where V_0 is the velocity of the plane front in an isotropic medium with diffusion coefficient D and θ is the angle between the propagation direction and the x axis. We note that a different and erroneous expression for $V_0(\theta)$ was given in Ref. 89.

In the primed coordinate system the autowave front is described by the natural equation $K' = K'(l')$. From the definition of curvature

$$K'(l') = -\frac{d\alpha'}{dl'}, \tag{7.3}$$

where α' is the angle of inclination of the tangent to the x' axis. It is not difficult to obtain the following equation for the coordinates of an element of the front in the laboratory system:[20]

$$x = x_0 + \int_0^{l'}\cos\left(\alpha_0' - \int_0^{\xi_1'}K'(\xi_2')d\xi_2'\right)d\xi_1', \qquad y = y_0 + \frac{1}{\lambda}\int_0^{l'}\sin\left(\alpha_0' - \int_0^{\xi_1'}K'(\xi_2')d\xi_2'\right)d\xi_1', \tag{7.4}$$

where x_0, y_0 are the coordinates of the free edge in the laboratory system and α_0' is the angle between the tangent to the front at the end point and the x' axis. These equations are essentially parametric equations of a curve, where the parameter is the arc length l' in the primed coordinate system. Knowing the parametric representation of the front, its curvature can be calculated in the usual way. For example, the time dependence of the curvature as we approach the end point is given by

$$K_0(t) = \lambda^2 K_{cr}[1 + (\lambda^2 - 1)\cos^2(\omega_0 t + \phi)]^{-3/2}. \tag{7.5}$$

Figure 10 (from Ref. 20) shows the calculated motion of a spiral wave in an anisotropic medium described by (7.1) with $D = 1$ and $D_1 = 2$. We see that the shape of the front is not in a steady state and undergoes periodic changes.

In spite of the fact that the curvature of the front depends on time, we can still refer to steady-state circulation of a spiral wave in an anisotropic medium, since the core of the wave (which has the shape of an ellipse with semi-axes R_0 and R_0/λ) remains fixed.

We next consider the non-steady-state effects associated with the evolution of spiral waves in a medium whose anisotropy varies in time. We first study the motion of a spiral wave in the case of a sudden change in the anisotropy of the medium. Suppose a steady spiral wave rotates in an

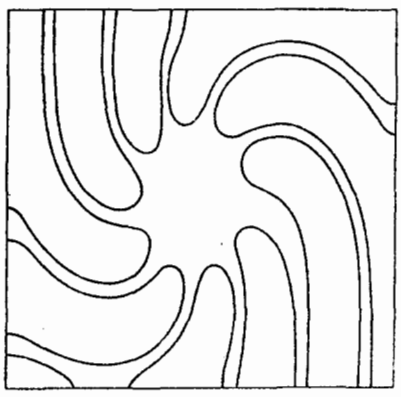

FIG. 10. Successive positions of a spiral wave in the model (7.1) of an anisotropic excitable medium. $D = 1$, $D_1 = 2$.

isotropic medium (7.1) with diffusion coefficient $D_1 = D$ when $t < 0$ and at $t = 0$ there is an instantaneous change in the anisotropy of the medium so that $D_1 = D + \Delta D$ for $t > 0$, where $\mu = \Delta D / D \ll 1$.

At time $t = 0$ the curvature of the front near the free edge of the spiral wave is $K_0 = K_{cr}$. This initial value will then relax toward the "steady state" value (7.5) in an anisotropic medium. The resulting core displacement is not difficult to calculate in the quasi-steady-state approximation:[20]

$$\Delta x_0 = \frac{\mu V_0}{2\omega_0} F_1\left(\frac{\gamma}{D}, p, \alpha_0\right), \quad \Delta y_0 = \frac{\mu V_0}{2\omega_0} F_2\left(\frac{\gamma}{D}, p, \alpha_0\right), \tag{7.6}$$

where

$$F_1 = \sin^2\alpha_0 \cdot \cos\alpha_0 - \Phi \frac{(\gamma/D)\sin\alpha_0 + \cos\alpha_0}{(\gamma/D)^2 + 1},$$
$$F_2 = \sin^3\alpha_0 + \Phi \frac{(\gamma/D)\cos\alpha_0 - \sin\alpha_0}{(\gamma/D)^2 + 1} \tag{7.7}$$
$$\Phi = \left(3 - 2p^{1/2}\frac{\gamma}{D}\right)\left(1 - \frac{3}{2}\cos^2\alpha_0\right).$$

In (7.6) and (7.7) we have omitted higher-order terms that are small as a result of the condition $p \equiv DK_{cr}/V_0 \ll 1$.

Similarly, we can determine the displacement of the center of the core of a spiral wave when the anisotropic medium (7.6) transforms suddenly into an isotropic medium with diffusion coefficient D:

$$\Delta x_0 = -\frac{\mu V_0}{2\omega_0} F_1\left(\frac{\gamma}{D}, p, \alpha_0\right), \quad \Delta y_0 = -\frac{\mu V_0}{2\omega_0} F_2\left(\frac{\gamma}{D}, p, \alpha_0\right). \tag{7.8}$$

Suppose now that the diffusion coefficient in the y direction is given by

$$D_1 = D - \frac{\Delta D}{2}\left[1 + \operatorname{sign}(\sin\omega_1 t)\right], \tag{7.9}$$

where $|\omega_1 - \omega_0| \ll \omega_0$. Because of the periodic jumps in the anisotropy, the displacements of the core center resulting from single jumps will accumulate and the end point will move along a trajectory determined by the equations (for $\mu \ll 1$)

$$\frac{dx}{dt} = \frac{\mu V_0}{2\pi} F_1\left(\frac{\gamma}{D}, p, \alpha_0 + (\omega_0 - \omega_1)t\right),$$
$$\frac{dy}{dt} = \frac{\mu V_0}{2\pi} F_2\left(\frac{\gamma}{D}, p, \alpha_0 + (\omega_0 - \omega_1)t\right). \tag{7.10}$$

In particular, in the case of perfect resonance ($\omega_1 = \omega_0$) the center of circulation will move along a straight line with the velocity

$$U = \frac{\mu V_0}{2\pi}\left[F_1^2\left(\frac{\gamma}{D}, p, \alpha_0\right) + F_2^2\left(\frac{\gamma}{D}, p, \alpha_0\right)\right]^{1/2}. \tag{7.11}$$

We note that in contrast to resonance in an isotropic medium, where the core center moves with a constant velocity for any α_0, the velocity in an anisotropic medium depends essentially on the phase α_0.

But this is not the only distinguishing feature of resonance in an anisotropic medium. Indeed, integration of (7.10) shows[20] that the trajectory of the core center in this case is not a circle or an ellipse, but a quite erratic curve. A series of typical trajectories are shown in Fig. 11 for different values of the ratio γ/D and $p = 0$. It is important to note that changes in the initial phase α_0 and the absolute value of the frequency difference $|\omega_0 - \omega_1|$ do not lead to changes in the shapes of the trajectories, but only affect their positions (but not orientations) in the plane and their geometrical dimensions.

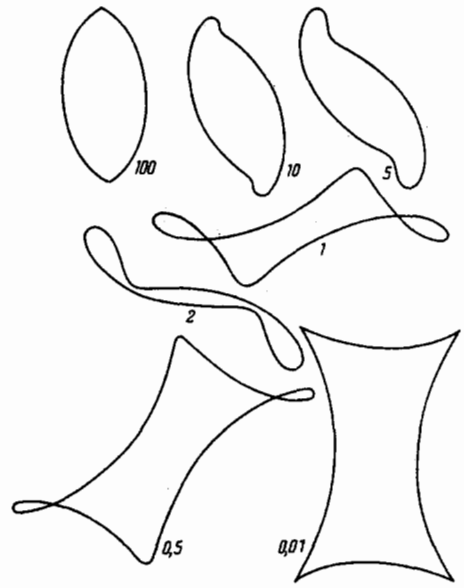

FIG. 11. Resonance trajectories obtained in the kinematic model of the motion of an autowave with modulation of the degree of ansiotropy of the medium, as indicated by the values of γ/D, and with $p = 0$.

It is interesting to compare the results of the kinematic treatment of the motion of a spiral wave in an excitable medium with periodically modulated anisotropy to the calculations of the reaction–diffusion model (7.1), in which the diffusion coefficient has the form (7.9). Figure 12a shows the trajectory of the center of the spiral wave for $\Delta D = 0.2$ and $\omega_1 = 0.12$. We note that for the medium modeled here the propagation velocity V_0 and circulation frequency ω_0 measured in the computer simulations are $V_0 = 1.3$ and $\omega_1 = 0.11$. Since the diffusion coefficient $D \approx 1$, it follows from (4.6) and these values that $p = DK_{cr}/V_0 : p = 0.21$. As

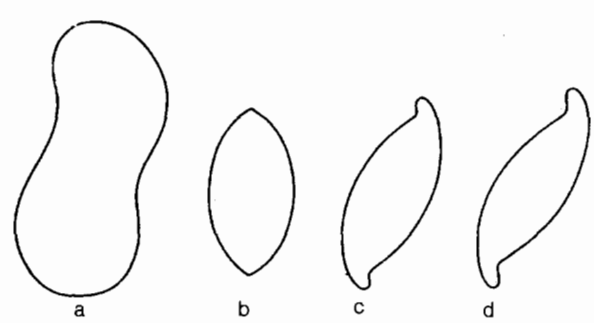

FIG. 12. Resonance trajectories obtained in the case of a periodic modulation of the degree of anisotropy in the model (7.1) (a) and in the kinematic model with $\gamma/d = 3.3$ (b), $\gamma/D = 6.0$ (c), and $\gamma/D = 9.0$ (d).

shown above, for a given value of p the form of the trajectory is determined only by the time lag γ/D, which is unknown. Three trajectories calculated from (7.10) for different values of γ/D are shown in Figs. 12b–d. We see that when $\gamma/D = 3.3$ the trajectory no longer has concave sections, as in Fig. 12a. Concave sections appear for larger values of γ/D (see Fig. 12c and 12d) but the trajectory shown in Fig. 12d has too large of an inclination with respect to the y axis. By comparing Figs. 12a and 12c it can be seen that the kinematic approach gives the correct qualitative picture of resonance in an anisotropic medium. In addition, the results can be used to estimate γ/D. For example, $\gamma/D = 6$ for the medium modeled here.

8. SPIRAL WAVES ON CURVED SURFACES

The basis for the study of kinematics of autowave structures on curved surfaces is (3.16), which was derived in Ref. 11. We first consider steady circulation of a spiral wave on the surface of a sphere of radius R_0, whose Gaussian curvature is constant and equal to $\Gamma = 1/R_0^2$. In the steady-state case we can integrate (3.16) once. Using (3.8), we have

$$K\int_0^l KV\,d\xi + \Gamma_0\int_0^l V\,d\xi - D\frac{dK}{dl} = A\,, \tag{8.1}$$

where A is an integration constant. Unlike the plane case, A is not the rotation frequency ω of the spiral wave, but is related to it as follows:

$$\omega^2 = A^2 + V_0^2\Gamma_0\,. \tag{8.2}$$

Suppose the radius of the sphere is so large that $R_0K_{cr} \gg 1$. Then the method of matching interior and exterior solutions used above to study spiral waves in a plane (see Sec. 4) can be extended without difficulty to the case of a spherical surface. The exterior solution of (8.1) can be obtained by neglecting the term $D\,dK/dl$ in (8.1), i.e. the dependence of the propagation velocity of the front on its curvature. Unlike the plane case, here there are two solutions: antisymmetric $K_a(l)$ and symmetric $K_s(l)$ with respect to the equator:[11]

$$K_a = \left(\frac{A}{V_0} - \Gamma_0 l\right)\left(\frac{2Al}{V_0} - \Gamma_0 l^2\right)^{-1/2}, \tag{8.3}$$

$$K_s = |K_a(l)| - \frac{2A}{V_0}\Gamma_0^{-1/2}\,\delta\left(1 - A(V_0\Gamma_0)^{-1}\right). \tag{8.4}$$

The delta function in the second term in (8.4) indicates that the front described by the symmetric solution $K_s(l)$ has a discontinuous slope on the equator at the point $l = A/V_0\Gamma_0$. The antisymmetric solution (8.3) is unphysical.[11]

We see from (8.3) that the curvature blows up when $l \to 0$ and $l \to 2A/V_0\Gamma_0$, i.e. near the north and south poles of the sphere. Hence the dependence of the wave velocity on geodesic curvature must be taken into account inside narrow layers near the poles. In other words, boundary layers must exist near the poles of the sphere. It follows from (8.1) that inside the north and south boundary layers the curvature is given by the following expressions:

$$K = K_{cr} - Al/D,\quad K = K_{cr} - A(L-l)/D\,, \tag{8.5}$$

where L is the total length of the front.

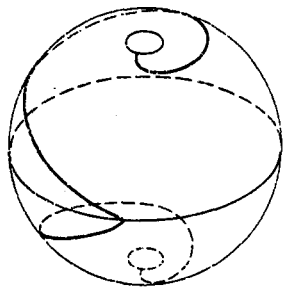

FIG. 13. Front of a spiral autowave on the surface of a sphere.

Therefore the front of a uniformly rotating spiral wave on a sphere is symmetric about the equatorial plane (Fig. 13). The wave has two cores located near the poles. Inside the boundary layers near the north and south poles the dependence of K on l is linear. If the dependence of the wave velocity V on the curvature K is linear, the discontinuity in the slope of the front on the equator disappears and there is a third boundary layer near the equator where the curvature is negative and depends on l quadratically.

From the matching conditions of the interior and exterior solutions near one of the cores, the integration constant A can be found and then (8.2) can be used to get the rotation frequency ω (Ref. 1):

$$\omega = \omega_0\left(1 + \frac{V_0^2}{2\omega_0^2}\Gamma\right) \equiv \omega_0\left(1 + \frac{V_0\Gamma_0}{2\xi^2 DK_{cr}^3}\right), \tag{8.6}$$

where ω_0 is the angular velocity of the spiral wave on a plane and is given by (4.12). Hence for a given excitable medium the angular velocity of rotation of a spiral wave on a sphere is larger than on a plane.

We note that recently the evolution of spiral waves on the surface of a sphere has been studied experimentally.[97] Spiral waves were excited in a solution with a Belousov–Zhabotinskiĭ chemical reaction on the surface of a small ($R_0 \approx 0.6$ mm) bead. The steady-state limit considered here was not observed during the experiment. Apparently this is due to the fact that the spherical surface used in the experiment was too small: one turn of the spiral barely fits on the surface. Also the dispersion produced by the medium was large (the typical width of a front on the photographs shown in Ref. 97 is comparable to the radius of the sphere) and in this case even on a plane non-steady-state (cycloid) rotation of spiral waves occurs,[33] which will be discussed below.

To study the evolution of spiral waves on a surface with variable curvature it is convenient to consider first the dynamics of a spiral wave on a sphere whose radius oscillates periodically in time according to the equation

$$R = R_0 + R_1\cos(\omega_1 t + \beta),\quad R_1 \ll R_0\,. \tag{8.7}$$

In this case the Gaussian curvature of the sphere oscillates with the amplitude $\Gamma_1 = 2R_1/R_0^3$. Let θ_0 and ϕ_0 be the polar and azimuthal angles of the center of the core of the spiral wave and let θ and ϕ be the spherical coordinates of the moving end point of the autowave front. For convenience we choose the polar axis of the spherical coordinate system so that the core center is near the equator $(\pi/2) - \theta_0 \ll 1$. In

addition, we consider the special case $D_E = D_g$ in (1.2) for which $\gamma = 0$. The calculations simplify considerably in this case, since $C = 0$, yet the qualitative picture of the evolution of the spiral wave is not changed significantly by this approximation.[1]

When $C = 0$ and $r_0 \ll R_0$ the velocity of the end point in spherical coordinates is given by the equations

$$\dot{\theta} = -\frac{V_0}{R}\sin\omega t, \quad \dot{\phi} = \frac{V_0}{R}\frac{\cos\omega t}{\sin\theta_0}. \tag{8.8}$$

Suppose the oscillation frequency of the radius of the sphere is close to the rotation frequency ω of the spiral wave: $|\omega - \omega_1| \ll \omega$. Substituting (8.6) [where Γ_0 is replaced by $\Gamma_0 - \Gamma_1\cos(\omega t + \beta)$] and (8.7) into (8.8) and averaging over time (i.e. only the slowly oscillating terms with frequency $|\omega_1 - \omega|$ are kept), we find that when the radius of the sphere is periodically modulated the center of the spiral wave drifts along the surface of the sphere with the following angular velocities

$$\dot{\theta}_0 = \frac{V_0 R_0 \Gamma_1}{4}\left(1 - \frac{1}{\xi^2}\frac{V_0}{DK_{cr}}\frac{\Gamma_0}{K_{cr}^2}\right)\sin[(\omega_1 - \omega)t + \beta],$$
$$\dot{\phi}_0 = \frac{V_0 R_0 \Gamma_1}{4\sin\theta_0}\left(1 - \frac{1}{\xi^2}\frac{V_0}{DK_{cr}}\frac{\Gamma_0}{K_{cr}^2}\right)\cos[(\omega_1 - \omega)t + \beta]. \tag{8.9}$$

As in the case of a periodic variation in the parameters of a plane excitable medium,[21,73] the drift is caused by resonance. The trajectory of the core center is a closed curve whose size increases as ω_1 approaches ω. When $\omega = \omega_1$ the direction of the drift is determined by the initial phase β of the modulation and the drift velocity is proportional to the amplitude of the variation in the Gaussian curvature Γ_1.

One would expect that spiral waves drift when they move along a surface with variable curvature, as in the case of a nonuniform medium (see Sec. 6). However, it can be shown[1] that on a surface with a constant Gaussian curvature, but with variable average curvature (examples are a cylinder, cone, and pseudosphere) drift does not occur. Therefore a nonuniform average curvature is not a sufficient condition for drift of a spiral wave, but a necessary condition for drift is a nonuniform Gaussian curvature.

We consider a spiral wave on a sphere whose surface is slightly deformed so that the Gaussian curvature Γ is a function of the polar angle θ. Since the deformation of the sphere is small, the Gaussian curvature Γ varies only slightly over a distance of the order of the core of a spiral wave and $d\Gamma/d\theta(r_0/R_0) \ll \Gamma_0$. When a spiral wave moves over such a nonuniformly curved surface, the end point successively passes through regions with different values of the Gaussian curvature. Therefore it moves as if the Gaussian curvature of the surface were time dependent:

$$\Gamma = \Gamma_0 + \frac{d\Gamma}{d\theta}\Big|_{\theta=\theta_0}\frac{r_0}{R_0}\cos\omega t. \tag{8.10}$$

Therefore the evolution of a spiral wave on a nonuniformly curved surface can be found by calculating the motion of a spiral wave on a spherical surface with a periodically varying radius, which was considered above. The time dependence of the curvature (8.7) is characterized in this case by the parameters

$$\Gamma_1 = \frac{d\Gamma}{d\theta}\Big|_{\theta=\theta_0}\frac{r_0}{R_0}, \quad \beta = 0, \quad \omega_1 = \omega.$$

For these values of the parameters we can obtain the drift velocities from (8.9) (Refs. 1 and 74):

$$\dot{\theta}_0 = 0,$$
$$\dot{\phi}_0 = \frac{V_0 r_0}{4\sin\theta_0}\left(1 - \frac{1}{\xi^2}\frac{V_0}{DK_{cr}}\frac{\Gamma_0}{K_{cr}^2}\right)\frac{d\Gamma}{d\theta}\Big|_{\theta=\theta_0}. \tag{8.11}$$

It follows from (8.11) that the drift velocity of a spiral wave along a nonuniformly curved surface is proportional to the absolute value of the gradient of the Gaussian curvature. Also the motion is perpendicular to the gradient of the curvature. We note that the term $V_0\Gamma_0/(\xi^2 DK_{cr}^3)$ inside the parentheses in (8.11) is small compared to unity, since it is of order $(r_0/R_0)^2$. Hence the sign of the angular velocity $\dot{\phi}_0$ is determined by the sign of $d\Gamma/d\theta$. For example, on the surface of a prolate spheroid a spiral wave rotating counterclockwise in the northern "hemisphere" should drift with angular velocity $\dot{\phi}_0 < 0$.

We estimate now the drift velocity for a medium with a Belousov–Zhabotinskiĭ reaction. We assume the typical values $V_0 = 3$ mm/min and $r_0 = 0.5$ mm. Suppose that the spiral wave rotates on the surface of a prolate spheroid with semiminor axis $a = 2$ mm and semimajor axis $b = 3$ mm and suppose that the center of the core corresponds to the angle $\theta_0 \approx \pi/6$. Using (8.11), we obtain the angular velocity $\dot{\phi} = 0.035$ min^{-1}, which corresponds to a drift velocity of $V_d \approx 0.04$ mm/min. Under these conditions the center of the spiral wave moves a distance of the order of the core radius after about 10 revolutions of the spiral wave.

The drift of spiral waves along nonuniformly curved surfaces has also been studied by computer simulations of the model (1.2) with the functions F and G in the form (1.3) and the coefficients $k_f = 1.7$, $k_g = 2$, $d = 0.1$, $\varepsilon = 0.15$, $k_\varepsilon = 6$, $\sigma = 0.01$, $D_E = D_g = 1$. The propagation velocity for this medium is $V_0 \approx 0.4$ and the core radius is $r_0 \approx 2$. The initial position of the center of the core was $\theta_0 \approx 0.56$ and $\phi_0 \approx 0.2$.

The calculated trajectory of the end point of the spiral wave is shown in Fig. 14. The elliptical form of the trajectory loops is an artifact of the use of angle coordinates. In metric coordinates the boundary of the core is a circle. We see from Fig. 14 that the core of the spiral wave drifts along the parallel of the spheroid ($\dot{\theta}_0 = 0$) in the direction given by (8.11). In addition, the drift velocity estimated from (8.11)

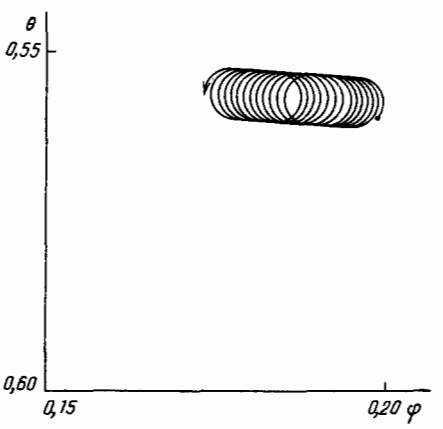

FIG. 14. Trajectory of the end point of a spiral wave on the surface of a prolate spheroid.

($\dot{\phi} = 2.8 \cdot 10^{-5}$) agrees fairly well with the numerical result ($\dot{\phi} = 3.6 \cdot 10^{-5}$).

The above results are even more important because it is now possible to observe this effect with the help of a modification of the Belousov–Zhabotinskiĭ reaction by means of an immobilized catalyst. In this modification the reaction proceeds only within a thin layer near the bottom, not over the entire volume of the solution. We recall that the resonance effects for spiral waves on a plane predicted in the framework of the kinematic approach[21,73] have already been confirmed experimentally.[3] This suggests that the drift effect should also exist and the estimates given here suggest that the displacement of the spiral wave should be observable visually. Therefore if the catalyst is immobilized on a nonuniformly curved surface of given topography, one has new possibilities for the control of spiral waves. In particular, it is possible to obtain motion of spiral waves in required directions, steady-state rotation in a certain region, or annihilation of pairs of spiral waves with opposite topological charges. It is very important that nonuniformity of the properties of the excitable medium, and this greatly simplifies the implementation of such methods of controlling spiral waves.

9. CYCLOID CIRCULATION

All the examples of the kinematic approach considered above assumed that the period of circulation of the spiral wave is much larger than the response time of the medium. Then the interaction between excitation pulses successively passing through a given point of the medium is small and can be neglected. However in the case of steady circulation of a spiral wave, a periodic train of curved wave fronts passes through each point of the excitable medium, except inside the core. This fact must be taken into account if the period of circulation is not sufficiently large.

Using the reasoning of Sec. 2 for single pulses,[39,130] we find that $V(K,T)$ is determined by the following generalization of (2.8):

$$V(K, T) = D_E K + V_p(\varepsilon^*, \varepsilon T), \tag{9.1}$$

where $V_p(\varepsilon,\varepsilon T)$ determines the propagation velocity of a train of waves with rectangular fronts and a period T between the waves. The dependence $K^*(T)$ was found in Ref. 39 for the model (1.2) with $D_g = 0$ and is shown in Fig. 15a. The dependence of the propagation velocity of the autowave on the curvature of the front K and the period T is shown in Fig. 15b for the model (1.2).

We assume as before that the propagation velocity of the wave front depends only on its curvature and the period T is a parameter characterizing this dependence, but is not related to ω. Then it follows from Sec. 4 that the angular velocity ω is given by (4.5) or (4.12) and depends only on two quantities: the velocity of a plane front V_p and the critical curvature $K_{cr} \approx K^*$. However, the quantities on the right hand sides of (4.5) and (4.12) are now functions of the period T between the waves, which is $T = 2\pi/\omega$ for steady circulation, where ω is the angular velocity of revolution of the wave. Hence (4.5) becomes a nonlinear algebraic equation for the angular velocity of the circulation

$$\omega = V_p^2\left(\varepsilon, \frac{2\pi\varepsilon}{\omega}\right) \psi K^*\left(\frac{2\pi}{\omega}\right)\left(V_n\left(\varepsilon, \frac{2\pi\varepsilon}{\omega}\right)\right)^{-1}. \tag{9.2}$$

As noted above, the functions $V_p(\varepsilon,\varepsilon T)$ and $K^*(T)$ in (9.2) can be found numerically or analytically (see Refs. 32, 50, 100, for example). In particular, the angular velocity of circulation can be calculated analytically by solving the algebraic equation (9.2).

It can be shown[31,32,40] that the right hand side of (9.2) falls off with increasing ω and hence it has a unique solution. The angular velocity will be smaller than in the absence of dispersion. This quantitative difference has been pointed out in many papers.[75,88,91,117,118]

However, the interaction between the turns of the spiral also leads to qualitatively new effects,[31–33,39,93,98,130] such as the loss of stability of circular circulation of a spiral wave and the onset of cycloid circulation, which has been observed in computer simulations[33] and in experiments using Belousov–Zhabotinskiĭ reactions.[113,123,126] The main feature of this case is that the trajectory of the free edge of a spiral wave propagating in a uniform and steady medium is no longer a circle, but forms a complicated curve resembling a cycloid.

The existence of cycloid circulation can be explained quite simply in the kinematic approach. As an illustration, we assume the simplest linear dependence for $V(K,T)$ and $K_{cr}(T)$:[34,39,130]

$$V(K, T) = V_0 + K - (V_0 - V_{cr})T_{min}T^{-1}, \quad K \geq K^*(T),$$
$$K_{cr}(T) = -(V_0 - V_{cr})(1 - T_{min}T^{-1}), \; V_{min} = \varkappa V_{cr} = V(K^*, T),$$
$$V_{cr} = V(K_{cr}, T). \tag{9.3}$$

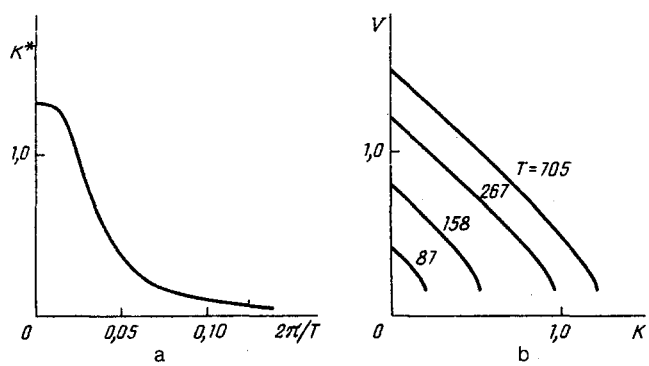

FIG. 15. Critical curvature K^* (a) and propagation velocity of the front V (b) in a periodic train of autowaves.

Here V_0 is the velocity of a single wave with a rectangular front and V_{min} is the minimum possible velocity for steady wave propagation.

As noted above, in steady circulation the wave fronts pass through all points of the medium with the same time interval T between fronts (equal to the period of circulation of the wave). In general, the time interval between waves may be different for different points of the medium and may also vary in time: $T = T(x,y,t)$. To construct the function $T(x,y,t)$, we note the instant of arrival of the preceding wave front at a given point of the medium $T^*(x,y,t)$. Then the function $T(x,y,t)$ in (9.3) is given by the simple expression

$$T = t - T^*[X(s, t), Y(s, t), t], \tag{9.4}$$

where $X(s,t)$ and $Y(s,t)$ are the Cartesian coordinates of the wave front.

The function $T(x,y,t)$ is calculated at the nodes of a square grid with a distance H between the nodes. Linear interpolation of $1/T$ is used between the nodes.

Two examples of the formation of a spiral wave from a semi-infinite rectangular front are shown in Fig. 16 for different values of the parameter T_{min}. The calculations were performed using the fundamental equation of kinematics (3.6), and the propagation velocity of the wave was calculated using (9.3) with $\theta_0 = 1.5$, $\theta_{cr} = 0.86$, $\varkappa = 0.9$, $\gamma = 5$, $H = 1$.

We see from Fig. 16 that the front gradually curves and then acquires a steady form and the trajectory of the end point becomes a circle. The radius of this circle and the rotation period are exactly the same as the calculated parameters for steady circulation. If T_{min} is small, then the period of circulation is close to the quantity T_0 determined by assuming that the velocity of the front depends only on its curvature. For the parameters chosen in Fig. 16 we have $T_0 = 34$.

As T_{min} increases, the period of circulation and the radius of the trajectory of the end point also increase. Upon further increase of T_{min} there is a qualitative change in the nature of the process and steady circulation becomes impossible. The angular velocity and the instantaneous radius of gyration of the end point are no longer constant, but oscillate. Hence the trajectory of the end point is no longer a circle, but resembles a cycloid (Fig. 17).

A simple qualitative explanation of cycloid circulation is as follows. In the case of steady circulation, the time between wave fronts (pulses) at all points of the medium is $T(x,y,t) = T_c$, where T_c is the period of circulation. But in the core of the spiral wave (bounded by the trajectory of the end point) the quantity $T(x,y,t)$ increases without bound as time goes on, since the wave front never enters this region of the medium.

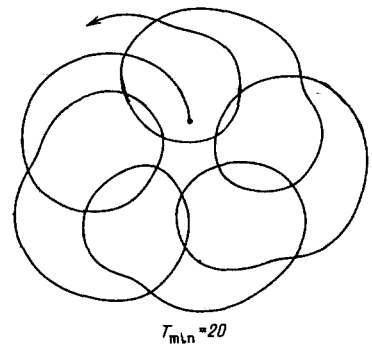

FIG. 17. Trajectory of the end point of the front in the kinematic model of the motion of an autowave for a large response time of the medium.

Therefore when $T_{min} \neq 0$ the circulation of the spiral wave creates a nonuniformity in the conditions of propagation of the front. For example, it follows from (9.3) that K_{cr} is different outside and inside the core. It was shown in Sec. 6 that a nonuniformity in the properties of the excitable medium results in a distortion of circular circulation. However, in the case considered here, the nonuniformity is of a specific type, and so under certain conditions circular circulation of the spiral wave is stable.

We assume that in an excitable medium with $T_{min} \neq 0$ a spiral wave is established with circular circulation. Because of a random fluctuation, the end point of the wave falls into the core, where K_{cr} is different. This leads to a displacement of the end point in the tangential direction (i.e. toward the center of the core) with velocity C [see (3.7)]. The rate of change of the curvature of the front at the end point obeys the following equation [see (3.7) and (5.3)]:

$$\frac{\partial K_0}{\partial t} = \gamma \frac{\partial K}{\partial l}\Big|_{l=0}(K_{cr} - K_0). \tag{9.5}$$

But the quantity K_{cr} also varies near the free edge of the spiral, since the end point moves into a region where the medium is nonuniform and $\partial K_{cr}/\partial r = \partial K_{cr}/\partial l$ (here r is the distance to the core center):

$$\frac{\partial K_{cr}}{\partial t} = \gamma \frac{\partial K_{cr}}{\partial l}\Big|_{l=0}((K_{cr} - K_0). \tag{9.6}$$

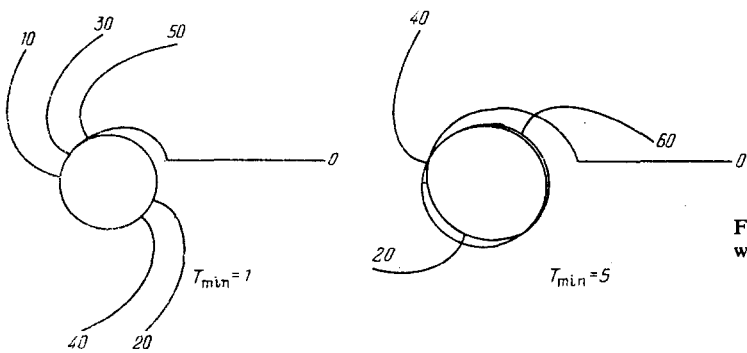

FIG. 16. Formation of a spiral wave in the kinematic model of a spiral wave for different response times of the medium.

It can easily be shown[35,39] that the solution of (9.5) and (9.6) is stable when

$$\frac{\partial K_{cr}}{\partial l}\Big|_{l=0} < \frac{\partial K}{\partial l}\Big|_{l=0}. \tag{9.7}$$

This inequality is a sufficient condition for circular circulation of the spiral wave to be stable. Indeed, if (9.7) is satisfied then the velocity C of tangential displacement of the end point decreases with time to zero, and the penetration length of the end point into the core varies directly with the amplitude of the initial fluctuation. In the opposite case even a small fluctuation can lead to a significant distortion in the trajectory of the end point. This condition has been verified by computer simulations of the kinematic model (3.6).[39]

10. THREE-DIMENSIONAL AUTOWAVE STRUCTURES

Some three-dimensional autowave structures can be described analytically.[45,54,90,118,127] The kinematic approach developed for two-dimensional excitable media can also be extended to the three-dimensional case and can be used to treat the dynamics of different autowave structures from a unified point of view.

As before, we assume that the autowave is completely specified by its front surface. Any surface in three-dimensional space has at each point two principal radii of curvature R_1 and R_2 (or two principal curvatures: $K_1 = 1/R_1$ and $K_2 = 1/R_2$). It was shown in Ref. 10 that the velocity of normal displacement of a part of the front depends only on the sum of the principal curvatures, i.e. on twice the average curvature $2H = K_1 + K_2$:

$$V = V_0 - 2DH. \tag{10.1}$$

The front can expand or contract along its edge (if it exists). The velocity C of this tangential growth depends not only on the average curvatures of the front near the edge, but also on the geodesic curvature $\varkappa$ of the edge itself:

$$C = \gamma_1(K_{cr} - 2H) - \gamma_2\varkappa, \tag{10.2}$$

where γ_1 and γ_2 are positive numbers; the curvature $\varkappa$ is taken as positive if the edge at a given point is convex with respect to the front.

The coefficient γ_1 is analogous to γ, which determines the velocity of growth of the end point of the front in a two-dimensional medium. But the coefficient γ_2 occurs only in the three-dimensional case. Like the other kinematic parameters, γ_2 can be determined by solving the "microscopic" equations (1.2). In addition, it can be shown[10] that if the diffusion coefficients of the activator and inhibitor are close ($D_E \to D_g = D$), then $\gamma_2 \to D$. Recall that in this case $\gamma_1 \to 0$.

We apply the kinematic approach to calculate the evolution of some three-dimensional autowave structures.

A spiral wave rotating on a plane can be considered as a plane cross section of a cylindrical surface. This surface is the simplest three-dimensional autowave structure: a rotating roll. A vortex of this kind is analogous to a spiral wave. The vortex core is a cylinder whose axis is called the thread of the roll.

The thread of the roll may be curved. In particular, it may be closed into a circle and then we have a vortex ring (Fig. 18a). Such structures are observed experimentally[121,123,125,126] and also in computer simulations[45,106,126] using models of the reaction—diffusion type.

A vortex ring is a local autowave source; it creates spherical diverging waves at large distances from its center. Computer calculations show[54] that, depending on the parameters of the excitable medium, a vortex ring can either shrink or expand while moving in the direction perpendicular to the plane of the thread. The velocity of this motion decreases with increasing radius R of the thread of the ring. In particular, an analytical treatment of the evolution of a vortex ring in a two-component model for identical diffusion coefficients shows[54,57] that the velocity of compression of the thread of a vortex ring is proportional to D/R. Therefore the quasi-steady-state kinematic approach discussed above can be used to treat the evolution of a ring vortex when its thread is only slightly curved.

We introduce cylindrical coordinates (x,ρ,φ) with the z axis along the symmetry axis of the vortex ring. Because of the cylindrical symmetry of the problem, it is sufficient to consider the evolution of a section of the vortex ring in the ρ, z plane, i.e. its meridian (Fig. 18b). Since the meridian lies in a plane, its evolution is obviously described by the fundamental kinematic equation (3.6). However, unlike the case of a spiral wave on a plane, the velocity of normal displacement of the meridian and the velocity of tangential growth of the end point will depend not only on its curvature. Indeed, (10.1) shows that the velocity of normal displacement is determined by the average curvature, which is not difficult to calculate for the meridian

$$H = \frac{1}{2}(K - \rho^{-1}\sin\alpha), \tag{10.3}$$

where ρ is the distance of an element of the front from the z axis and α is the angle between the tangent to the meridian of the ring and the ρ axis (see Fig. 18b).

The tangential curvature of the edge of the front surface is

$$\varkappa = -\rho_0^{-1}\cos\alpha_0; \tag{10.4}$$

where α_0 and ρ_0 are the values of the angle α and distance ρ at the end point of the meridian. It follows from the definition of the curvature that

$$\alpha = \alpha_0 - \int_0^l K dl'. \tag{10.5}$$

Since, as emphasized above, the angular velocity in the quasi-steady-state case is determined by the form of the front near the free edge of the spiral wave, we need only study the motion of that part of the surface of the vortex ring which is right next to the core.

The motion of the end point of the meridian is determined by the equations

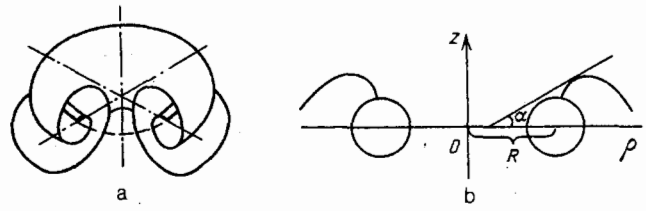

FIG. 18. Vortex ring in a three-dimensional excitable medium (a) and axial cross section of the vortex ring (b).

$$\frac{d\rho_0}{dt} = -V(l=0)\sin\alpha_0 - C\cos\alpha_0,$$
$$\frac{dz_0}{dt} = V(l=0)\cos\alpha_0 - C\sin\alpha_0, \tag{10.6}$$

which are analogous to (3.10). In addition, (3.11) also remains valid

$$\frac{d\alpha_0}{dt} = \frac{dV}{dl}\Big|_{l=0} + CK_0. \tag{10.7}$$

It follows from (3.8), (10.3), and (10.4) that the quantity $\partial V/\partial l$ is given by the expression

$$\frac{\partial V}{\partial l} = D\frac{\partial K}{\partial l} - DK\frac{\cos\alpha}{\rho}. \tag{10.8}$$

Substituting (10.1), (10.3), and (10.8) into (3.6), we obtain the equation

$$\frac{\partial}{\partial l}\left[K_0\int^l K(V_0 - DK)dl - D\frac{\partial K}{\partial l}\right] = \frac{\partial K}{\partial t} + \left(C - D\frac{\cos\alpha_0}{R}\frac{\partial K}{\partial l}\right). \tag{10.9}$$

It follows from (10.9) that (5.3), which describes the quasi-steady-state case in a two-dimensional medium, is modified as follows for the case of a vortex ring:

$$\frac{dK_0}{dt} = -\left(C - D\frac{\cos\alpha_0}{R}\right)\frac{\partial K}{\partial l}\Big|_{l=0}. \tag{10.10}$$

Taking into account these differences, (5.7) and (5.9) can be written in the form

$$\dot{K}_0 = \xi\left(\frac{V_0}{D}\right)^{1/2}$$
$$\times\ [\gamma_1(K_{cr} - K_0 + R^{-1}\sin\alpha_0) + R^{-1}(\gamma_2 - D)\cos\alpha_0]K_0^{3/2},$$
$$\dot{\alpha}_0 = \xi\left(\frac{V_0}{D}\right)^{1/2} K_0^{3/2} - DK_0R^{-1}\cos\alpha_0 + K_0[\gamma_2R^{-1}\cos\alpha_0$$
$$+ \gamma_1(K_{cr} - K_0 + R^{-1}\sin\alpha_0)]. \tag{10.11}$$

The system of equations (10.11) completely determines the dependence of the angle α_0 and curvature K_0 on time in the quasi-steady-state case. Integrating these equations, substituting the solution into (10.6), and averaging over a period of circulation, we obtain the following equations for the time dependence of the thread of the vortex ring:

$$\frac{dR}{dt} = \frac{3V_0}{4K_{cr}}\frac{(\gamma_1/D)^2 + [(\gamma_2 - D)/D]}{(\gamma_1/D)^2 + 1}\frac{1}{R} - \frac{D}{R}, \tag{10.12}$$

$$\frac{dz_0}{dt} = -\frac{3V_0\gamma_1}{4RK_{cr}D}\frac{(\gamma_2 - D)/D - 1}{(\gamma_1/D)^2 + 1} - \frac{V_0}{DK_{cr}}\frac{\gamma_2 - D}{2\xi R}. \tag{10.13}$$

Recall that we have assumed a vortex ring of large radius in a medium with low excitability ($DK_{cr} \ll V_0$), and therefore we have omitted terms of higher order in R^{-1} in the above expressions, as well as small terms in $p \equiv DK_{cr}/V_0 \ll 1$ and in $\gamma_1/D \ll p^{-1/2}$ (the quasi-steady-state condition).

For the special case of a two-component excitable medium with indentical diffusion coefficients we have[10] $\gamma_2 = D$ and $\gamma_1 = 0$. Substituting these values into (10.12) and (10.13), we obtain

$$dR/dt = -D/R, \quad dz/dt = 0,$$

which agrees with the numerical results and with analytical results obtained by a different method.[54] Hence a vortex ring is practically always unstable. It either shrinks ($\dot{R} < 0$) or expands ($\dot{R} > 0$) with time.

There exists, however, a narrow interval of values of the parameters in which the rate of change of R is very small and passes through zero. Inside this interval higher order terms in $1/R$ must be taken into account in the expression for $\dot{R}$. Detailed analysis shows[49] that a term of order $1/R^2$ does not exist, while a term of order $1/R^3$ appears in the expression for $\dot{R}$ with a positive coefficient. Therefore, if the vortex ring shrinks in the linear approximation in $1/R$, but its velocity of compression is very small, the nonlinear positive term of order $1/R^3$ may be able to compensate the compression and stabilize the vortex ring.

In addition, numerical calculations show[10,126] that small vortex rings of stable size can be observed. The stabilization mechanism in this case is the interaction between wave fronts colliding on the symmetry axis of the vortex ring.

The evolution of a vortex ring can be controlled by means of a periodic modulation in the properties of the excitable medium. For example, if the critical curvature K_{cr} depends on time according to (6.1) with $\omega_1 = \omega_0$, then a collapsing ring can be forced to expand and also to reverse its drift direction along the z axis by properly choosing the amplitude and phase of the modulation. It is interesting that a proper choice of K_1 and ϕ can simultaneously stabilize the size of the ring and stop its drift, i.e. completely stabilize the ring.[2] Depending on the parameters of the excitable medium, this equilibrium position may be either stable or unstable.

Although the above estimates apply directly only to the evolution of a circular vortex ring, they can be used as a first approximation to describe the time behavior of any vortex with an arbitrarily curved thread, as long as the curvature is not very strong. Indeed, a small element of an arbitrary vortex will appear to be part of a vortex ring of an appropriate radius.[10] Suppose initially we have a line vortex (cylindrical roll) and we apply a small local deformation of the thread. If the parameters of the medium are such that vortex rings tend to shrink, the deformation will tend to decrease with time. In the opposite case, when vortex rings expand, any deformation of the thread blows up and the vortex thread tends to become longer. As a result, a straight cylindrical roll becomes unstable to small deformations of its thread and very complicated structures can be formed in an infinite excitable medium.

These qualitative features of the dynamics of three-dimensional autowave vortices can be formulated mathematically. For example, a system of kinetic equations for the evolution of three-dimensional autowave structures was proposed in Refs. 90 and 92. These equations are based on the dependence of the velocity of the thread on its shape.

Finally we discuss the properties of twisted vortices, which differ from straight vortices in that the edge is a helical curve coiled around the cylindrical core (Fig. 19). A twisted vortex can be characterized quantitatively by the parameter $\mu = 2\pi/h$, where h is the pitch of the helix. For a nonuniformly twisted vortex a more convenient definition is

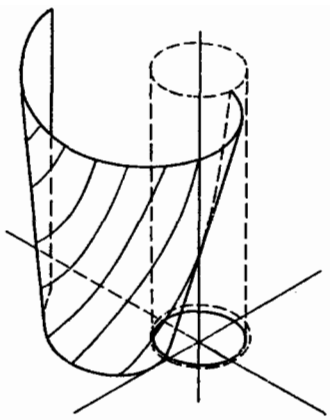

FIG. 19. Twisted cylindrical vortex in a three-dimensional excitable medium.

$\mu(z) = d\alpha/dz$, where α is the azimuthal angle determining the position of an element of the helical edge on the cylindrical core. Depending on whether the edge forms a right or a left helix, the torsion μ will be positive or negative, respectively.

The front surface of a uniformly twisted vortex is a helicoid. We consider a section of the helicoid formed by the plane $z = \text{const}$. Its evolution is obviously described by (3.6), where K is the curvature of the section and in our approximation V does not depend on μ (the first correction to the velocity because of torsion is proportional to μ^2).

Since $\mu = \text{const}$, the shape of the section $z = \text{const}$ does not depend on time. Therefore in the linear approximation in μ the angular velocity of rotation of a twisted vortex can be found by calculating the rotation of a spiral wave on a plane. The rotation frequency of the twisted vortex is therefore given by (4.10) with K_{cr} replaced by $K(0)$, where $K(0)$ is the curvature of the section near the vortex core. The curvature $K(0)$ is found by setting the growth velocity C equal to zero. Using the standard methods of the theory of surfaces,[52] we obtain[12] that the average curvature of the helicoid as we approach the core is $H(0) = 1/2K(0)$, while the tangential curvature of the edge is $\varkappa = |\mu|$. Substituting these curvatures into (10.2) and equating C to zero, we obtain the curvature $K(0)$ of the section:

$$K(0) = K_{cr} + |\mu|\gamma_2\gamma_1^{-1}. \tag{10.14}$$

From (10.14) and (4.9) we can obtain an expression for the angular velocity of rotation of a twisted vortex

$$\omega = \omega_0\left(1 + \frac{3}{2}\frac{\gamma_2}{\gamma_1}\frac{1}{K_{cr}}|\mu|\right) \tag{10.15}$$

and the core radius

$$R = R_0\left(1 - \frac{3}{2}\frac{\gamma_2}{\gamma_1}\frac{1}{K_{cr}}|\mu|\right). \tag{10.16}$$

Therefore the angular velocity of rotation of a twisted vortex is higher than in the case of a simple roll. The increase in the rotation frequency was observed in computer simulations,[45] however the explanation of this phenomenon given in Ref. 45 was based on the unfounded assumption that the core radius of a twisted vortex is the same as for an untwisted vortex. This assumption leads to a quadratic dependence of ω on μ rather than a linear dependence.

We note that the motion of a uniformly twisted vortex was considered in Ref. 101 in the Rinzel–Keller model and it was shown there that the angular velocity of rotation increases because of the twist.

We turn now to the dynamics of nonuniformly twisted vortices. Suppose that $\mu = f(z)$ at the initial time. We see from (10.15) that different parts of the vortex with different values of μ will rotate with different velocities, and hence the torsion varies in time. Using (10.15), it is not difficult to obtain an equation describing the dependence of μ on z and the time t:

$$\frac{\partial\mu}{\partial t} = u(\operatorname{sign}\mu)\frac{\partial\mu}{\partial z}, \tag{10.17}$$

where $u = (3/2)(\gamma_2/\gamma_1)\omega_0/K_{cr}$. This unusual nonlinear equation belongs to the class of equations describing so-called kinematic waves,[6] and its solution is of the form

$$\mu = f(z + (\operatorname{sign}\mu)ut). \tag{10.18}$$

The solution (10.18) shows that if the vortex is twisted nonuniformly at the initial time, torsional waves will propagate along it. Initial torsional perturbations with opposite signs propagate along the vortex in opposite directions with velocity u and form discontinuities (or shock waves) when they collide.

11. CONCLUSION

It is evident from the present review that the kinematic approach is an effective and quite general method of studying the evolution of different autowave structures. Its domain of applicability is obviously not limited to the typical examples discussed above. The techniques of the kinematic approach are useful in studying the evolution of autowaves in nonuniform and at the same time non-steady-state media, in nonuniform or non-steady-state three-dimensional media, and other combinations of the "elementary" situations considered above. The kinematic approach can be used to study the behavior of spiral waves near the boundary of an excited region and to describe the interactions between spiral waves. Another important problem is also the improvement of the kinematic treatment of cycloid types of circulation of spiral waves.

The kinematic approach can be used not only to consider spiral waves analytically, but also as a powerful method of numerical analysis of autowave structures, since the kinematic equations are much simpler than the original reaction–diffusion system of equations.

It is also important to note that the ideas on which the kinematic approach is based have already been used to work out alternative methods of describing excitable media. For example, interest in the model of an excitable medium as a network of cellular machines has been revived.[36,80,81,96] The cell models strive to reproduce to the maximum degree the kinematics of autowaves motion, especially the effect of the form of the front on the propagation velocity.

Meanwhile, there is also the possibility of further refinements of the kinematic approach using the ideas and results of alternative approaches.

This cross-fertilization of ideas will undoubtedly lead to progress in understanding the formation and evolution of autowave structures.

[1] A. Yu. Abramychev, V. A. Davydov, and V. S. Zykov, Zh. Eksp. Teor. Fiz. **97**, 1188 (1990) [Sov. Phys. JETP **70**, 666 (1990)].
[2] A. Yu. Abramychev, V. A. Davydov, and A. S. Mikhaĭlov, Biofizika **34**, 979 (1990). [Biophys. (USSR) **34**, (1990)].
[3] K. I. Agladze, V. A. Davydov, and A. S. Mikhaĭlov, Pis'ma Zh. Eksp. Teor. Fiz. **45**, 601 (1987) [JETP Lett. **45**, 767 (1987)].
[4] I. S. Aranson and M. I. Rabinovich, "Dynamics of spiral waves in nonuniform media" (In Russian), Preprint IAP, No. 212, Gor'kiĭ, 1988.
[5] I. S. Balakhovskiĭ, Biofizika **10**, 1063 (1965). [Biophys. (USSR) **10**, 1175 (1965)]
[6] Yu. I. Balkareĭ, M. G. Nikulin, and M. I. Elinson, in: Autowave Processes in Systems with Diffusion [in Russian], IAP, Gor'kiĭ, 1981.
[7] W. Barton, M. Cabrera, and F. Frank, *Elementary Processes of Crystal Growth* [Russ. transl., IL, M., (1959)].
[8] V. P. Belousov, *Sbornik Referat. Radiats. Meditsin.*, 1958, (In Russian) Medgiz., M., 1959; Autowave Processes in Systems with Diffusion [in Russian], IAP, Gor'kiĭ, 1981.
[9] M. B. Berkinblum, S. A. Kovalev, V. V. Smolyaninov, and L. M. Chaĭlakhyan, *Models of Structural and Functional Organization of Biological Systems* [in Russian], Nauka, M., 1966; p. 71.
[10] P. K. Brazhnik, V. A. Davydov, V. S. Zykov, and A. S. Mikhaĭlov, Zh. Eksp. Teor. Fiz. **93**, 1725 (1987) [Sov. Phys. JETP **66** 984 (1987)].
[11] P. K. Brazhnik, V. A. Davydov, and A. S. Mikhaĭlov, Teor. Mat. Fiz. **74**, 440 (1988). [Theor. Math. Phys. (USSR) **74**, 300 (1988)].
[12] P. K. Brazhnik, V. A. Davydov, and A. S. Mikhaĭlov, Izv. Vyssh. Uchebn. Zaved. Radiofiz. **32**, 289 (1989) [Radiophys. Quantum Electron. **32**, (1989)].
[13] A. I. Buzdin and A. S. Mikhaĭlov, Zh. Eksp. Teor. Fiz. **90**, 294 (1986) [Sov. Phys. JETP **63**, 169 (1986)].
[14] V. A. Vasil'ev, Yu. M. Romanovskiĭ, and V. G. Yakhno, Usp. Fiz. Nauk **128**, 625 (1979) [Sov. Phys. Usp. **22**, 615 (1979)].
[15] V. A. Vasil'ev, Yu. M. Romanovskiĭ, and V. G. Yakhno, *Autowave Processes* [in Russian], Nauka, M., 1987.
[16] A. B. Vasil'eva and V. F. Butuzov, *Asymptotic Expansions of the Solutions of Singular Perturbed Equations* [in Russian], Nauka, M., 1973.
[17] I. M. Gel'fand and M. L. Tsetlin, Dokl. Akad. Nauk SSSR **131**, 1242 (1960) [Sov. Math. Dokl. **1** (1960)].
[18] S. I. Gel'fand and D. A. Kazhdan, Dokl. Akad. Nauk SSSR **141**, 527 (1961) [Sov. Math. Dokl. **2** (1961)].
[19] Yu. V. Gulyaev, Yu. D. Kalafati, L. A. Ryabova, and I. A. Serbinov, Dokl. Akad. Nauk SSSR **256**, 357 (1981) [Sov. Phys. Dokl. **26**, 52 (1981)].
[20] V. A. Davydov and V. S. Zykov, Zh. Eksp. Teor. Fiz. **95**, 139 (1989) [Sov. Phys. JETP **68**, 80 (1989)].
[21] V. A. Davydov, V. S. Zykov, A. S. Mikhaĭlov, and P. K. Brazhnik, Izv. Vyssh. Uchebn. Zaved. Radiofiz. **31**, 574 (1988). [Radiophys. Quantum Electron. **31** (1988)].
[22] V. A. Davydov and A. S. Mikhaĭlov, *Nonlinear Waves. Structures and Bifurcation* [in Russian], Nauka, M., 1987.
[23] E. A. Ermakova, A. M. Pertsov, and É. É. Shnol', Dokl. Akad. Nauk SSSR **301**, 332 (1988) [Sov. Phys. Dokl. **33**, 519 (1988)].
[24] A. M. Zhabotinskiĭ, *Concentration Self-Excited Oscillations* [in Russian], Nauka, M., 1974.
[25] A. M. Zhabotinskiĭ, K. Otmer, R. Field *et al.*, *Oscillations and Travelling Waves in Chemical Systems* [Russ. transl., Mir, M., 1988].
[26] Ya. B. Zel'dovich, *Nonlinear Waves. Propagation and Interaction*, (In Russian) Nauka, M., 1981; p. 38.
[27] Ya. B. Zel'dovich and D. A. Frank-Kamenetskiĭ, Dokl. Akad. Nauk SSSR, **19**, 693 (1938).
[28] V. S. Zykov, *Control of Complex Systems* [in Russian] Nauka, M., 1975, p. 59.
[29] V. S. Zykov, Biofizika **25**, 319 (1980). [Biophys. (USSR) **25**, 329 (1980)].
[30] V. S. Zykov, Biofizika **25**, 888 (1980). [Biophys. (USSR) **25**, 906 (1980)].
[31] V. S. Zykov, in *Autowave Processes in Systems with Diffusion* [in Russian], IAP, Gor'kiĭ, 1981 p. 85.
[32] V. S. Zykov, *Simulation of Wave Processes in Excitable Media* [in Russian], Nauka, M., 1984.
[33] V. S. Zykov, Biofizika **31**, 862 (1986). [Biophys. (USSR) **31**, 940 (1986)].
[34] V. S. Zykov, Biofizika **32**, 337 (1987). [Biophys. (USSR) **32**, 365 (1987)].
[35] V. S. Zykov, Biofizika **34**, 1031 (1989). [Biophys. (USSR) **34**, 1114 (1989)].
[36] V. S. Zykov and A. S. Mikhaĭlov, Dokl. Akad. Nauk SSSR **286**, 341 (1986) [Sov. Phys. Dokl. **31**, 51 (1986)].
[37] V. S. Zykov and O. L. Morozova, Biofizika **24**, 717 (1979). [Biophys. (USSR) **24**, 739 (1979)].
[38] V. S. Zykov and O. L. Morozova, Biofizika **25**, 1071 (1980). [Biophys. (USSR) **25**, 1100 (1980)].
[39] V. S. Zykov and O. L. Morozova, "The kinematic treatment of the stability of spiral autowaves," (In Russian) Preprint Inst. of Problems in Control, Moscow, 1988.
[40] V. S. Zykov, O. L. Morozova, and V. R. Pratusevich, Vopr. Kibern. No. 93, 43 (1982).
[41] V. S. Zykov and A. A. Petrov, Biofizika **22**, 300 (1977). [Biophys. (USSR) **22**, 307 (1977)].
[42] G. R. Ivanitskiĭ, V. I. Krinskiĭ, and E. E. Sel'kov, *Mathematical Biophysics of Cells* [in Russian], Nauka, M., 1978.
[43] A. N. Kolmogorov, I. G. Petrovskiĭ, and N. S. Piskunov, Byull. Mosk. Univ. Sek. A **1**(6), 1 (1937); Vopr. Kibern. No. 12, 3 (1975).
[44] V. I. Krinskiĭ, Probl. Kibern. No. 20, 59 (1968).
[45] B. I. Krinskiĭ, A. B. Medvinskiĭ, and A. V. Panfilov, *Evolution of Autowave Vortices* [in Russian], Znanie, M., 1986.
[46] V. I. Krinskiĭ and A. S. Mikhaĭlov, *Autowaves* [in Russian], Znanie, M., 1984.
[47] V. I. Krinskiĭ, A. M. Pertsov, and A. N. Reshetilov, Biofizika **17**, 271 (1972). [Biophys. (USSR) **17**, 282 (1972)].
[48] S. P. Kurdyumov and G. G. Malinetskiĭ, *Synergetics: The Theory of Self-Organization. Ideas, Methods, and Perspectives* [in Russian], Znanie, M., 1983.
[49] A. Yu. Doskutov and A. S. Mikhaĭlov, *Introduction to Synergetics* [in Russian], Nauka, M., 1990.
[50] A. S. Mikhaĭlov and V. I. Krinskiĭ, Biofizika **27**, 875 (1982). [Biophys. (USSR) **27**, 919 (1982)].
[51] G. Nicolis and I. Prigogine, *Self-Organization in Non-Equilibrium Systems*, Wiley, N.Y., 1977 [Russ. transl., Mir, M., 1979].
[52] A. P. Norden, *Theory of Surfaces* [in Russian], Gostekhizdat, M., 1956.
[53] L. A. Ostrovskiĭ and V. G. Yakhno, Biofizika **20**, 489 (1975). [Biophys. (USSR) **20**, 498 (1975)].
[54] A. V. Panfilov, A. N. Rudenko, and V. I. Krinskiĭ, Biofizika **31**, 850 (1986). [Biophys. (USSR) **31**, 926 (1986)].
[55] L. S. Polak and A. S. Mikhaĭlov, *Self-Organization in Nonequilibrium Physical and Chemical Systems* [in Russian], Nauka, M., 1983.
[56] P. K. Rashevskiĭ, *Course of Differential Geometry* [in Russian], Fizmatgiz, M., 1956.
[57] Yu. M. Romanovskiĭ, N. V. Stepanova, and D. S. Chernavskiĭ, *Mathematical Biophysics* [in Russian], Nauka, M., 1984.
[58] A. N. Rudenko and A. V. Panfilov, Stud. Biophy. **98**, 183 (1983).
[59] Yu. M. Svirezhev, *Nonlinear Waves, Dissipative Structures, and Catastrophes in Ecology* [in Russian], Nauka, M., 1987.
[60] E. Scott, *Waves in Active and Nonlinear Media in Electronics* [Russian translation], Sov. Radio, Moscow (1977).
[61] G. B. Whitham, *Linear and Nonlinear Waves*, Wiley Interscience, N.Y., 1974. [Russ. transl., Mir, M., 1977].
[62] D. A. Frank-Kamenetskiĭ, *Diffusion and Heat Transfer in Chemical Kinetics* [in Russian], Nauka, M., 1967.
[63] H. Haken, *Introduction to Synergetics*, Springer-Verlag, N.Y., 1977. [Russ. transl., Mir, M., 1980].
[64] W. Ebeling, *Strukturbildung Bei Irreversiblen Prozessen* [in German], Teubner, Leipzig, 1976 [Russ. transl., Mir, M., 1979].
[65] K. I. Agladze and V. I. Krinsky (Krinskiĭ), Nature (London) **296**, 424 (1982).
[66] M. A. Allessie, F. I. M. Bonke, and F. J. G. Schopman, Circ. Res. **33**, 54 (1973).
[67] R. C. Brower, D. A. Kessler, J. Koplik, and H. Levine, Phys. Rev. Lett. **51**, 1111 (1983).
[68] R. C. Brower, D. A. Kessler, J. Koplik, and H. Levine, Phys. Rev. A **29**, 1335 (1984).
[69] J. Bures, V. I. Koroleva, and N. A. Gorelova, in: Self-Organization: Autowaves and Structures far from Equilibrium, ed. by V. I. Krinsky, Springer-Verlag, Berlin, 1984; p. 180.
[70] R. Casten, H. Cochen, and P. Langerstrom, Quart. J. Appl. Math. **32**, 365 (1975).
[71] D. S. Cohen, J. C. Neu, and R. R. Rosales, SIAM J. Appl. Math. **35**, 536 (1978).
[72] J. M. Davidenko, P. F. Kent, D. R. Chialo, D. C. Michaels, and J. Jalife, "Sustained vortex-like waves in normal isolated ventricular muscle", Reprint, Dept. of Pharmacology and Physiology, SUNY, Health Science Center at Syracuse, NY (1990).
[73] V. A. Davydov, A. S. Mikhaĭlov, and V. S. Zykov, in *Nonlinear Waves in Active Media*, ed. by Yu. Engelbrecht, Springer-Verlag, Berlin (1989); p. 38.
[74] V. A. Davydov and V. S. Zykov, Nonlinear World, Naukova Dumka, Kiev (1989); Vol. 1, p. 81.
[75] J. D. Dockery, J. P. Keener, and J. J. Tyson, Physica D **30**, 177 (1988).
[76] P. C. Fife, in *Non-Equilibrium Dynamics in Chemical Systems*, Eds. C. Vidal and A. Pacault, Springer-Verlag, Berlin (1984); p. 76.
[77] P. C. Fife, J. Stat. Phys. **39**, 687 (1985).
[78] R. FitzHugh, Biophys. J. **1**, 445 (1961).
[79] P. Foerster, S. C. Muller, and B. Hess, Science **241**, 685 (1988).

[80] M. Gerhardt, H. Schuster, and J. J. Tyson, Science **247**, 1563 (1990).
[81] M. Gerhardt, H. Schuster, and J. J. Tyson, Physica D **46**, 392 (1990).
[82] G. Gerisch, Wilhelm Roux Archiv Entwickelungsmech. Organismen, **165**, 127 (1965).
[83] N. A. Gorelova and J. Bures, J. Neurobiology **14**, 353 (1983).
[84] J. M. Greenberg, SIAM J. Appl. Math. **39**, 301 (1980).
[85] J. M. Greenberg, Adv. Appl. Math. **2**, 450 (1981).
[86] P. S. Hagan, SIAM J. Appl. Math. **42**, 762 (1982).
[87] R. N. Hramov, A. N. Rudenko, A. V. Panfilov, and V. I. Krinsky, Stud. Biophys. **102**, 69 (1984).
[88] J. P. Keener, SIAM J. Appl. Math. **46**, 1039 (1986).
[89] J. P. Keener, J. Math. Biol. **26**, 41 (1988).
[90] J. P. Keener, Physica D **31**, 269 (1988).
[91] J. P. Keener and J. J. Tyson, Physica D **21**, 307 (1986).
[92] J. P. Keener and J. J. Tyson, Physica D **44**, 191 (1990).
[93] B. Ya. Kogan, V. S. Zykov, and A. A. Petrov, *Simulation of Systems '79*, North-Holland, Amsterdam (1980); p. 693.
[94] E. Lugosi, Physica D **40**, 331 (1989).
[95] G. H. Markstein, J. Aeronaut. Sci. **18**, 199 (1951).
[96] M. Markus and B. Hess, *Dissipative Structures in Transport Processes and Combustion*, Springer-Verlag, Berlin (1990); p. 123.
[97] J. Maselko and K. Showalter, Nature (London) **339**, 609 (1989).
[98] E. Meron, Phys. Rev. Lett. **63**, 684 (1989).
[99] E. Meron and P. Pelce, Phys. Rev. Lett. **60**, 1880 (1988).
[100] A. S. Mikhailov and V. J. Krinsky, Physica D **9**, 346 (1983).
[101] A. S. Mikhailov, A. V. Panfilov, and A. N. Rudenko, Phys. Lett. A **109**, 246 (1985).
[102] S. C. Muller, T. Plesser, and B. Hess, Science **230**, 661 (1985).
[103] S. C. Muller, T. Plesser, and B. Hess, Physica D **24**, 71 (1987).
[104] S. C. Muller, T. Plesser, and B. Hess, Physica D **24**, 87 (1987).
[105] J. Nagumo, S. Arimoto, and S. Yoshizawa, Proc. IRE **50**, 2061 (1962).
[106] P. J. Nandapurkar and A. T. Winfree, Physica D **29**, 69 (1987).
[107] A. M. Pertsov, A. V. Panfilov, and E. A. Ermakova, Physica D **14**, 311 (1984).
[108] J. Rinzel and J. B. Keller, Biophys. J. **13**, 1313 (1973).
[109] A. Rosenblueth, Am. J. Physiol. **194**, 491 (1958).
[110] O. E. Rossler and C. Kahlert, Z. Naturforsch. Teil A **34**, 565 (1979).
[111] A. B. Rovinsky, J. Phys. Chem. **90**, 217 (1986).
[112] O. Selfridge, Arch. Inst. Cardiol. Mexico **18**, 177 (1948).
[113] G. S. Skinner and H. L. Swinney, Physica D **45**, 287 (1990).
[114] R. Sultan and P. J. Ortoleva, J. Chem. Phys. **84**, 6781 (1986).
[115] A. M. Thuring, Phil. Trans. Roy. Soc. (London) B **237**, 37 (1952).
[116] J. J. Tyson, K. A. Alexander, V. S. Manoranjan, and J. D. Murray, Physica D **34**, 193 (1989).
[117] J. J. Tyson and J. P. Keener, Physica D **29**, 215 (1987).
[118] J. J. Tyson and J. P. Keener, Physica D **32**, 327 (1988).
[119] N. Wiener and A. Rosenblueth, Arch. Inst. Cardiol. Mexico **16**, 3 (1946).
[120] A. T. Winfree, Science **175**, 634 (1972).
[121] A. T. Winfree, Science **181**, 937 (1973).
[122] A. T. Winfree, Sci. Am. **230**(6), 82 (1974).
[123] A. T. Winfree, "The geometry of biological time," in *Biomathematics*, Vol. 8, Springer-Verlag, N.Y., 1980.
[124] A. T. Winfree, Physica D **12**, 321 (1984).
[125] A. T. Winfree, *When Time Breaks Down*, Princeton Univ. Press (1987).
[126] A. T. Winfree and W. Janke, J. Phys. Chem. **93**, 2823 (1989).
[127] L. V. Yakushevich, Stud. Biophys. **100**(3), 195 (1984).
[128] A. N. Zaikin and A. M. Zhabotinsky (Zhabotinskiĭ), Nature (London), **225**, 535 (1970).
[129] V. S. Zykov, in *Simulation of Wave Processes in Excitable Media*, Translation ed. by A. T. Winfree, Univ. Press, Manchester (1988).
[130] V. S. Zykov and O. L. Morozova, Nonlinear Biology **1**(2), 1 (1990).

Translated by J. D. Parsons